Interim Report **R&D Project 357/1/T**

Development of Distributed Flood Forecasting Models using Weather Radar and Digital Terrain Data

R.J. Moore, V. Bell, G.A. Roberts
and D.G. Morris
Institute of Hydrology
December 1992

EXECUTIVE SUMMARY

The availability of spatial estimates of rainfall from weather radar on a square grid has prompted the development of rainfall-runoff models which are structured to share the same grid. This report shows how the problem of parameterisation of such models can be overcome through the use of contour maps, or digital terrain models (DTMs). "Linkage functions" are used to relate a grid parameter, whose value is required for many grids, to only one or two regional parameters and grid values which can be obtained from DTMs or maps. A routing function is derived from contour maps or DTMs via an extension of the classical isochrone concept. Runoff production employs a saturation excess principle with absorption capacity linked to the average slope within each grid square, again measured from contour maps or DTMs.

The simple advection-based isochrone method of flow routing is extended to incorporate diffusion, and implemented as a routing rather than convolution operation with computational speed advantages. This has been achieved through the use of a discretised kinematic wave formulation, each reach corresponding to an isochrone strip and receiving lateral inflow as direct runoff generated from grid squares located within the strip. A "Catchment Climbing" algorithm developed for use with the DTM is used to define flow path distances and time of travel to the catchment outlet. This has required the specification of different velocity models, including a form which employs slope as part of a Chezy-Manning relation. A particularly important advance made is the transfer of DTM path information to the distributed model: this allows velocity to be estimated as part of the model calibration process resulting in turn in optimised isochrones and improved forecast performance.

Slope is used as the main control on soil absorption capacity, affecting runoff generation, within the model. In addition, analysis of Landsat imagery is used to obtain a land cover classification for the study catchments and the urban fraction used to introduce a partial impervious area. Extensions, for example, to accommodate forest/grass effects on evaporation are planned.

Three catchments for model calibration and assessment are selected: the Wyre at St. Michaels in North West England, the Mole at Kinnersley Manor in the Thames basin and the Rhondda at Trehafod in South Wales. A preliminary database containing rainfall, flow and evaporation data for these catchments is implemented and preliminary model results obtained for two of the three catchments. These results show, when the radar data are of good quality, that significant model improvement is obtained by replacing data from a single raingauge by 2 km grid square radar data: 83% explained variance compared to 55% for the 126 km^2 Mole catchment. Further work is planned to extend the database, to perform more exhaustive model evaluation and to experiment with different forms of model.

ACKNOWLEDGEMENTS

Particular thanks are due to: George Merrick, NRA coordinator to the project, for his support and encouragement and for acting as chairman of steering committee meetings; Bryony May for her role as secretary to the steering committee; and Dan Cadman and Ian Pearce for support and data provision concerning the Welsh and North West case studies, respectively.

At the Institute of Hydrology Rob Flavin is thanked for his help in supplying the Digital Terrain Model (DTM) for model development. Marianne Polarski also assisted initially in setting up the DTM database on the modelling computer and in providing an initial form of the Catchment Climbing algorithm. Roger Austin supported the database management of rainfall, runoff and evaporation data and the model calibration shell software. Dawn Hotchkiss carried out work on radar rainfall preprocessing to remove anomalies in the radar data.

CONTENTS

1. INTRODUCTION

The traditional approach to modelling the response of a river basin to rainfall is through a lumped representation in which an estimate of catchment average rainfall is used as input. This traditional approach still persists as the most commonly employed approach, particularly for real-time flood forecasting applications. In such applications it is common to require only a forecast at a "basin outlet" location which is gauged and there is little interest in forecasts at internal locations or in a form of model parameterisation capable of predicting the effect of land-use change. Experience has shown that with adequate calibration data in the form of flow records and with only a sparse sampling of the rainfall field using raingauges that more complex, and possibly more realistic, distributed models fail to provide improved forecast accuracy. A common diagnosis is that the models are "input limited" and that improved performance from distributed models will only be achieved when better measurements of rainfall fields are used as input data. Such measurements are now available in the form of weather radar data, commonly available on a 2 km grid at 5 minute intervals.

The aim here is to develop a simple distributed rainfall-runoff model suitable for use in real-time flow forecasting with weather radar providing the source of rainfall input. Whilst it is neither natural nor essential to configure such a model on the radar grid it is the approach which will be investigated here. Such an approach is by no means new: an early example is provided by Anderl et al (1976). The methodology adopted here was first outlined at a symposium in 1987 (Moore, 1991) and preliminary results presented at workshops in 1990 and 1991 (Moore, 1992; Moore and Bell, 1993). Other workers have pursued similar lines, but with different model parameterisations, most notably Chander and Fattorelli (1991). For a recent review of simple distributed conceptual rainfall-runoff models for use with digital terrain data, but not specifically for use with weather radar data, see Polarski (1992).

The first year of the Study has focussed on developing tools for parameterising simple distributed models using digital terrain data. Section 2 presents the basic form of model used for the first trials. This is based on a simple soil water accounting procedure within each 2 km radar grid square and an advection-based routing model based on the isochrone concept. An extension to incorporate diffusion through a discrete kinematic wave formulation is developed and its convolution form replaced by a computationally more efficient routing operation. A parallel system of routing is invoked to accommodate flow along fast near surface paths and slow subsurface paths. Section 3 outlines the form of the Digital Terrain Model (presented in greater detail in Appendix A) and describes the "Catchment Climbing" algorithm used to derive fundamental flow path properties for use in rainfall-runoff model parameterisation. In particular, this includes the automatic derivation of isochrones by defining flow paths throughout the catchment and using velocity models and the length of flow paths to infer time of travel to the basin outlet. Inference of an optimal velocity is carried out as an integral part of the rainfall-runoff model calibration process by automatic optimisation. Velocity models considered include slope-dependent forms based on Chezy-Manning and a simple fixed velocity. The effect of land use on runoff production can be important and is considered in Section 4. Landsat images are used to classify land cover over the Study catchments and ways of incorporating these data into the distributed model formulation are then considered along with a more distributed form of the model. Evaluation of the different variants of the basic form of distributed flow forecasting model is addressed in Section 5. The characteristics of the three main Study basins - the Wyre at St. Michaels,

the Rhondda at Trehafod and the Mole at Kinnersley - are first described along with the data available for model calibration and evaluation. Preliminary results are then presented for two of the three Study catchments. Finally, Section 6 provides a summary of the main conclusions obtained so far and an indication of work planned for the second year of this two year Study.

2. MODELLING APPROACH

2.1 The basic form of model

In developing a distributed model suitable for operational use in real-time it is clear that a form of parameterisation is needed that does not involve a large number of parameters in need of optimisation. This dichotomy between the need for distributed parameters and a small number of them needing to be optimised will be resolved here through the use of contour maps, in the form of digital terrain models (DTMs) and simple "linkage functions". Contour maps are used in two ways. Firstly, the classical isochrone concept is used to "route" water to the basin outlet, essentially through dictating appropriate time delays as a function of travel paths across hillslope and down river channel pathways. Secondly, the slope of the terrain within a grid-square is used as a control on "runoff production", that is water available for routing rather than absorption by the soil/bedrock. Figure 2.1 provides a simple illustration of these two components which are expanded on below.

The construction of isochrones - lines joining points of equal time of travel to the basin outlet - is achieved in the basic form of the model by assuming that water travels with only two velocities depending on whether it is associated with a hillslope or in a river channel. In this way it is relatively easy to construct isochrones by direct inference from the distance of a point to the basin outlet. More complex rules will be introduced later, for example including slope influences via a flow resistance equation with the help of a DTM of the catchment. Figure 2.1(b) illustrates a pattern of isochrones superimposed on the radar grid used as the model grid. The areas between isochrones associated with each grid square are calculated and used to apportion runoff from the grid square to a given time delay. In this way a runoff-distributed convolution is achieved to derive the basin flow response at future times.

Formally the convolution of grid-square runoff rate per unit area over a grid square, $r_{t,j}$, from grid squares $j=1,2,\ldots,m$, to obtain the basin runoff rate per unit area over the basin, Q_t, at time t may be achieved using

$$Q_t = \sum_{j=1}^{m} \sum_{\tau=1}^{n} u_{\tau,j} \; r_{t-\tau,j} \qquad (2.1)$$

where $u_{\tau,j} = A_{\tau,j}/A$, $A_{\tau,j}$ is the area between the τ-1 and τ isochrones in the j'th radar grid square and A is the total basin area. Note the distributed form of this "unit hydrograph"; for uniform rainfall throughout the basin the underlying classical unit hydrograph is $v_\tau = A_\tau/A$, where $A_\tau = \Sigma_{j=1}^{m} A_{\tau,j}$ is the area occupied by the τ'th isochrone strip. The relation between $u_{\tau,j}$ and v_τ is $u_{\tau,j} = w_{\tau,j} v_\tau$ where $w_{\tau,j} = A_{\tau,j}/A_\tau$ for $\tau = 1,2,\ldots,n$ and $j = 1,2,\ldots,m$. The grid-square runoff rate, $r_{t,j}$, can be chosen to be the direct runoff rate, $q_{t,j}$, or the sum of this and baseflow, that is $r_{t,j} = q_{t,j} + b_{t,j}$. Experience with this simple time-area form of routing has subsequently led to the inclusion of additional storage elements to represent attenuation effects seen in observed hydrographs. These developments are discussed in Section 2.2.

Generation of runoff from a given grid-square is accomplished by conceptualising the grid-square as a box-shaped "soil" column. The key element in the conceptualisation is that the depth of the box, and thus the absorption capacity of the soil, is controlled by the average slope within the square as measured from the contour map or DTM. Specifically, the following

(a) River basin with superimposed weather radar grid

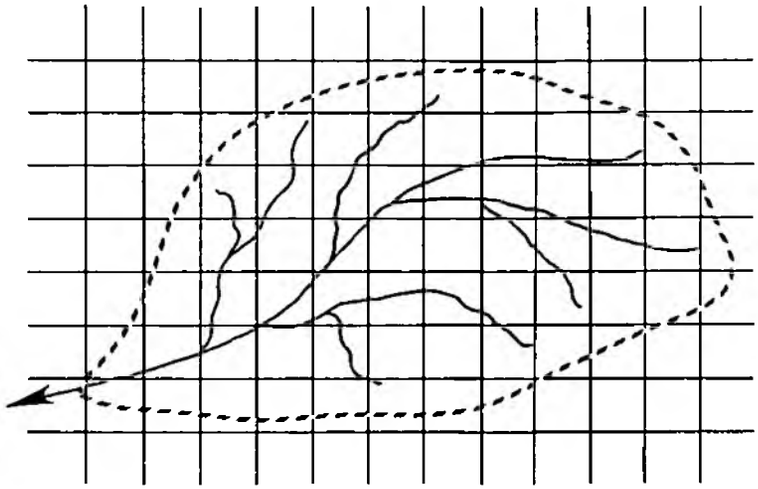

(b) Isochrones for grid-square j

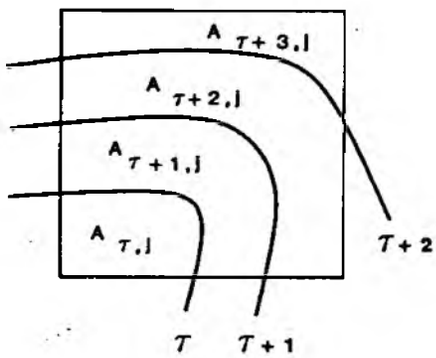

(c) Block representation of runoff response from grid-square j

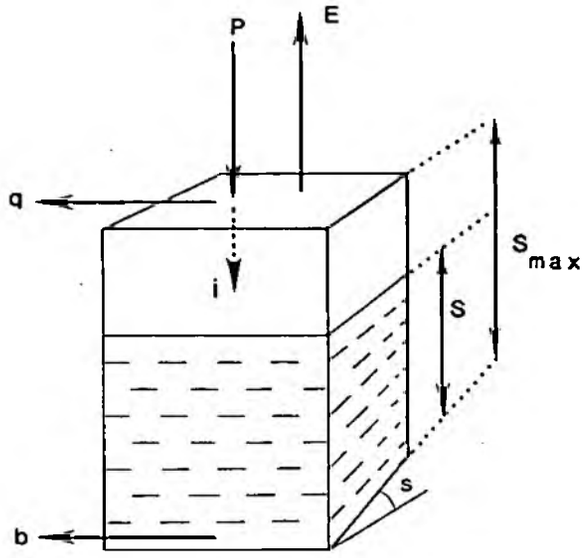

P: weather radar estimate of rainfall
E: evaporation
q: direct runoff
b: baseflow
S, S_{max}: water storage and maximum storage capacity
i: infiltration
s: average slope

Figure 2.1 Grid-square rainfall-runoff model for flood forecasting using radar data

linkage function is used to relate maximum storage capacity, S_{max}, to the average slope, s, within a grid-square:

$$S_{max} = \frac{(1 - s)}{s^*} S^*_{max} \quad . \tag{2.2}$$

The parameters s* and S^*_{max} are upper limits of slope and storage capacity respectively and act as "regional parameters" for the basin model. Clearly a measurement of slope for each grid square associated with the river basin can be made from the contour map or DTM whilst parameterisation is achieved for all grids using only these two parameters.

A water balance is maintained for each grid square by using the radar grid-square rainfall as input and introducing soil moisture dependent evaporation and drainage functions. Specifically the balance is maintained as follows for a given box and time interval (ignoring time and space subscripts for notational simplicity). Firstly, a soil moisture dependent infiltration function can be invoked for hydrological environments which experience infiltration-excess, as opposed to saturation-excess, runoff. A potential infiltration rate is given by

$$i_p = \left[1 - \frac{S}{S_{max}}\right]^b i_{max} \tag{2.3}$$

where i_{max} is the upper limit of infiltration rate and S is the water in storage. Then the actual infiltration rate is given by

$$i = \min(p, i_p) \tag{2.4}$$

where p is the rainfall rate. Then direct runoff by this infiltration excess mechanism is simply q = p - i. (In practice this component is not invoked for modelling the humid temperate basin use in the application that follows).

Drainage from the grid box occurs at the rate

$$b = \begin{cases} \alpha S^\beta & S > 0 \\ 0 & \text{otherwise} \end{cases} \tag{2.5}$$

where α is a storage constant (units of inverse time) and the exponent β is a parameter (set here to 3). Evaporation loss from the grid box occurs at the rate, E_a, which is related to the potential evaporation rate, E, through the relation

$$E_a = \begin{cases} \left[1 - \frac{D - D^*}{S_{max} - D^*}\right] E & D > D^* \\ E & D \le D^* \end{cases} \tag{2.6}$$

where D = S_{max} - S is the soil moisture deficit and D* is the threshold deficit below which

evaporation occurs at the potential rate.

The direct runoff rate is calculated as

$$q = \max(0, S\text{-}S_{max}) + p\Delta t - i\,\Delta t. \qquad (2.7)$$

and the updated water storage is given by $\max(0, S + i\Delta t - E_a\Delta t - b\Delta t)$.

2.2 Revised formulation of the basic model

The basic form of model developed in the previous sub-section was used in initial trials. However, two weaknesses were identified in the routing component of the model which led to further developments. The first was the computer time involved in computing the discrete form of convolution integral in equation (2.1), particularly as part of a parameter optimisation process. A second weakness was the pure form of advection routing implied by the use of the isochrone method and the need to introduce a diffusive element to obtain the more attenuated catchment response seen in practice.

A simple way of introducing diffusion into the isochrone formulation is to assume that each isochrone strip, instead of operating as a simple advection time delay, can be represented by a discrete kinematic wave. Specifically, the idea is to replace the n isochrone strips by a cascade of n reaches, with the outflow from the j'th reach at time k represented by

$$q_k^j = (1-\theta)\,q_{k-1}^j + \theta\,(q_{k-1}^{j-1} + r_k^j) \qquad (2.2.1)$$

where r_k^j is the direct runoff generated from the j'th isochrone strip in the interval (k-1, k) and θ is a dimensionless wave speed parameter. Moore and Jones (1978) show how this formulation may be derived from either a discrete form of the kinematic wave equation or a linear storage form of routing. In the case of the kinematic wave equation

$$\frac{\partial q}{\partial t} + \theta\frac{\partial q}{\partial x} = \theta r \qquad (2.2.2)$$

a simple finite difference approximation leads to

$$\left(q_k^j - q_{k-1}^j\right) + \theta\left(q_{k-1}^j - q_{k-1}^{j-1}\right) = \theta\, r_k^j. \qquad (2.2.3)$$

The model may also be derived from storage considerations by considering the storage S_k^j associated with the j'th node just before flows are transferred at time k. Continuity then gives

$$S_k^j = S_{k-1}^j + q_{k-1}^{j-1} - q_{k-1}^j + r_k^j \qquad (2.2.4)$$

and with the assumption of storage behaving as a linear reservoir

$$q_k^j = \theta\, S_k^j \qquad (2.2.5)$$

gives equation (2.2.1)

A first implementation of this model, following directly from the discrete convolution in the first form of model, used the model in impulse response function form along with equation (2.1). The impulse response function (here defined as the response to a unit input of direct runoff $r_k^n = 1$ k=n=0, =0 otherwise) of a cascade of n such kinematic wave elements is given by

$$u(n,k) = \begin{cases} \begin{bmatrix} k \\ n \end{bmatrix} (1-\theta)^{k-n}\theta^{n+1} & 0 \le n \le k \\ 0 & \text{otherwise} \end{cases} \qquad (2.2.6)$$

a function associated with binomial expansions. It is convenient, and efficient, to calculate this function in recursive form as

$$u(n,k) = \begin{cases} \dfrac{k(1-\theta)}{k-n}\, u(n,k-1) & k = n+1, n+2, \ldots \\ \theta^{n+1} & k = n \\ 0 & k < n \end{cases} \qquad (2.2.7)$$

for n $\geq$ 0. A plot of this impulse response function is shown in Figure 2.2(a) at selected reaches along an n-reach channel. The corresponding "distance response function" showing the response to an initial unit impulse along the channel, at specified times, can be computed using the following recursion:

$$u(n,k) = \begin{cases} 0 & n > k \\ \theta^{k+1} & n = k \\ \dfrac{t-n+1}{n}\, \dfrac{\theta}{1-\theta}\, u(n-1,k) & 0 \le n < k \\ (1-\theta)^k\theta & n = 0 \,. \end{cases} \qquad (2.2.7)$$

An example of the form of this distance response function is shown in Figure 2.2(b).

Trials with this revised formulation provided an improvement in modelling attenuation of the runoff through the catchment to its outlet. However, the convolution form of implementation is computationally expensive and a more efficient, and simpler, routing formulation has been adopted for use in subsequent work. This uses the discrete kinematic wave model in its original form of equation (2.2.1) with the direct runoff from the j'th isochrone strip over the interval (k-1, k) being obtained from

$$r_k^j = f \sum_{i=1}^{m} A_{j,i}\, r_{k,i} \qquad (2.2.9)$$

where $A_{j,i}$ is the area of the i'th radar grid square occupied by the j'th isochrone strip, $r_{k,i}$ is the direct runoff generated from this square and f is a units conversion factor (in the present

(a) **Impulse response function**

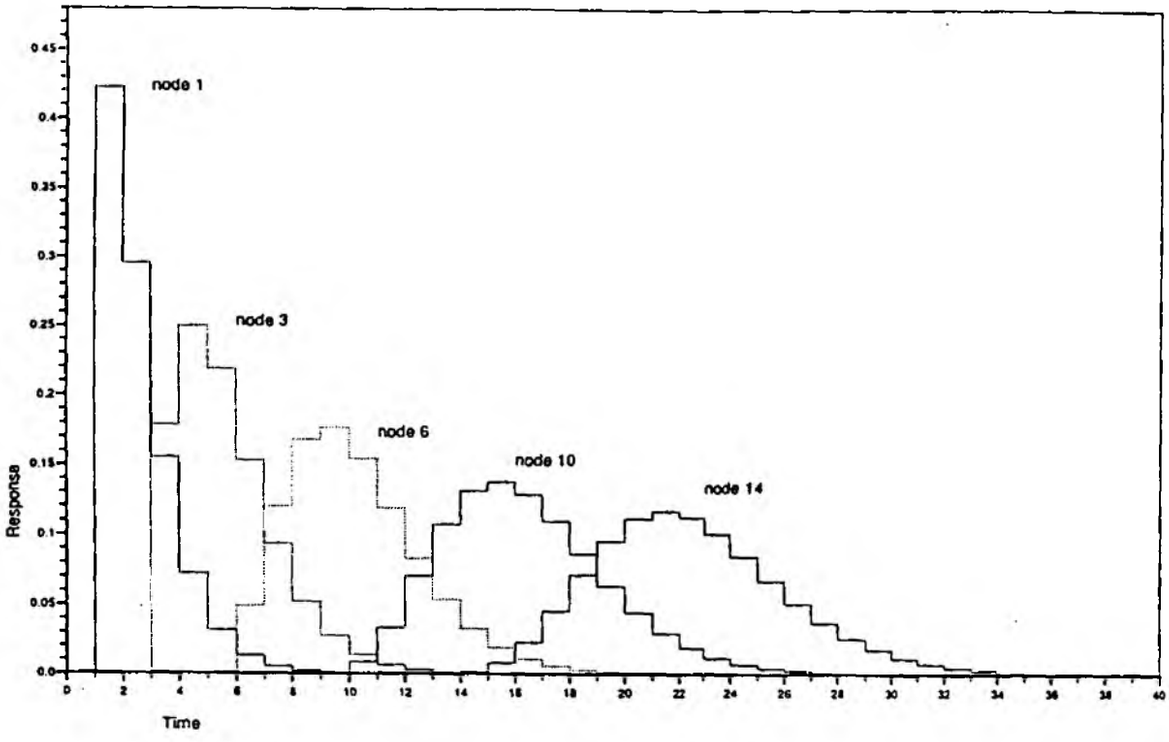

(b) **Distance response function**

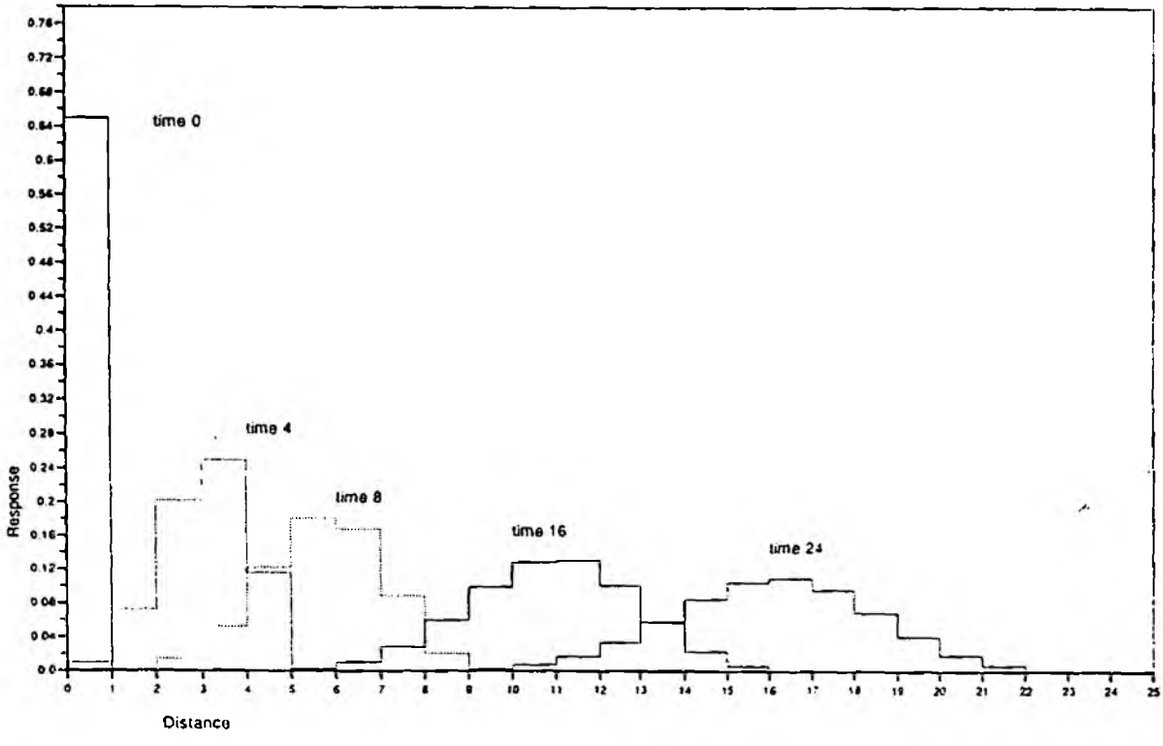

Figure 2.2 Response functions of the discrete kinematic wave model

case from km^2 mm/15 minutes to $m^3 s^{-1}$). This formulation results in a dramatic reduction in the computational needs of the model.

As previously mentioned in Section 2.1, $r_{k,i}$ can be defined as equal to direct runoff, $q_{k,i}$, or to be the sum of this and the baseflow, $b_{k,i}$. In the main form of the model an approach which routes direct runoff and baseflow separately using two parallel discrete kinematic wave models, having different wave speeds θ_s and θ_b, has been employed. The rainfall data may also be adjusted by a factor, c, to accommodate "calibration" errors prior to being used as grid-square rainfall.

The revised model formulation has been used as the basis of further extensions which exploit data from digital terrain models and Landsat land use classifications. These are described in later sections of this report.

3. MODEL PARAMETERISATION USING THE DTM

3.1 The DTM Algorithm

The Digital Terrain Model consists of five data types derived from 1:50000 Ordnance Survey source maps. The data values for each type are located at 50 metre grid intervals, with grid points lying on integer multiples of 50 metres, giving 400 grid points per square kilometre.

The five data types are:

(i) Ground elevation in units of 0.1 m;
(ii) Surface type, whether land, river, lake or sea;
(iii) Inflow drainage direction, a number between 0 and 254 indicating which of a points' eight near neighbours drain into it. It is not possible for all eight to flow into the same point;
(iv) Outflow drainage direction. Each point is allowed to drain in only one direction determined by the overland slope, ie. all the flow from a source point is assumed to travel to the neighbouring point with the lowest elevation below that of the source point;
(v) Cumulative Catchment Area expressed as the number of grid points that drain to a point, including that point itself. For example at the basin outlet, dividing the number of grid points by 400 will give the catchment area in km^2 units.

Further details of the DTM and its derivation are given in Appendix A. In essence a digital terrain model consists of a three dimensional representation of basin topography consisting of a large regular grid covering the basin, with elevation data at each grid point taken from Ordnance Survey 1:50000 maps. The four other data types listed above are then derived from this elevation data.

DTM data sets have been obtained for all basins used in this study: the Rhondda at Trehafod, the Thames basins (the Mole at Esher, Silkstream at Colindeep Lane and Yeading Brook at Yeading West) and the Wyre at St Michaels. The data are held on a Silicon Graphics workstation in the form of a direct access database, allowing easy retrieval via DTM database access software.

An algorithm associated with the DTM is fundamental to the derivation of the catchment data used to parameterise the distributed model. This "Catchment Climbing" algorithm calculates the boundary of the catchment draining to any point, needing only the x-y coordinates of the point in question and the DTM data as input. Starting at the outlet point, the algorithm works out from the inflow dataset which of the points eight near neighbours flows into it, and then moves to each one in turn. This process is repeated many times as the algorithm works its way up the catchment, until no more points are found to contribute to the flow at the outlet. The algorithm then forms a boundary to enclose the catchment. The process takes about 6 seconds cpu time on a Silicon Graphics workstation to work it's way up a 146 km^2 catchment, form the catchment boundary and produce a screen display.

3.2 Use of the DTM in Model Parameterisation

3.2.1 General

In the simplest formulation of the distributed model the DTM is used to supply a large data file for each catchment. This file contains, for each 2km radar square, slope data, isochrone data and the proportion of each radar square that lies in the catchment. The DTM is also used to supply various parameters such as catchment area, maximum slope and the length of unit hydrograph base.

The Catchment Climbing algorithm performs this function, working up the catchment from the outlet, numbering every point and recording details of each in the form of the northing and easting of the point, and the total distance travelled over both land and river to the outlet. To calculate these distances the algorithm searches through all previous points starting from the most recent to find the point the new point flows into. The distances travelled to the last point may now be obtained, and increased by 50m or 71m depending on whether the direction of flow is along the grid or diagonal to it. If the surface type is LAND the land distance is incremented, and for RIVER/LAKE the river distance is incremented. The information recorded enables the algorithm to produce details of every point containing the easting, northing, slope, travel time to outlet, height and land use. Here, slope is the slope of the land at that point calculated as

$$\sin\theta = \frac{y}{\sqrt{(y^2 + d^2)}} \qquad (3.2.1)$$

where y is the change in elevation between the point and the point it flows into, and d is the distance between the point and the point it flows into.

Travel time, τ, is calculated by keeping track of distances covered by land and river flow paths from a point to the outlet, assuming velocities for each and calculating the travel time to the outlet from

$$\tau = \frac{\ell_L}{v_L} + \frac{\ell_R}{v_R} \qquad (3.2.2)$$

where ℓ_L and ℓ_R are the distance travelled over land and river paths and v_L and v_R are the corresponding velocities. Velocity values of 0.5 m s^{-1} and 0.1 m s^{-1} for river and land paths have been assumed in initial trials of the model.

The land use data, referred to above have, been derived from Landsat satellite images and are discussed further in Section 4.

3.2.2 Derivation of Isochrones

The distributed model is configured on a 2km grid corresponding to the 2km radar rainfall grid. For each of these radar grid squares the model requires the following data:

(i) s_j - the average slope of grid square j,
(ii) c_j - the proportion of square j that lies in the catchment,
(iii) $w_{\tau j}$ - the proportion of square j that lies in the τth isochrone,
(iv) u_τ - the value of the τth time segment of the unit hydrograph.

These four data sets are derived from the output of the Catchment Climbing algorithm previously described as follows:

(i) The average slope s_j. This is found by taking the simple average of the slopes at the points lying in the jth square, resulting, not in the average slope of the radar grid square, but in the average slope of the flow paths in that square. This is considered a more valuable quantity since it is used in the model to determine how much rain contributes to rapid response runoff by controlling the storage capacity of that grid square.

(ii) The proportion of each radar grid square that lies in the catchment. This is determined by counting the number of DTM derived catchment points that lie in each 2km radar grid square and dividing by the maximum possible (1600). A value between zero and one is obtained.

(iii) The proportion of each radar grid square that lies in each isochrone. Currently a choice of hourly or quarter hourly isochrones is available, but this could be adapted readily for any time period. Note that w_{kj} determines the proportion of grid square j that lies in the kth isochrone (defined as being separated from the outlet by time τdt, where $k-1 \leq \tau < k$, and dt is the time separation between isochrones.) It has a value between zero and one.

(iv) The synthetic unit hydrograph. This is generated by calculating the area of each isochrone and dividing by the total area of the catchment. Again, areas are calculated simply by counting the number of DTM grid points in each isochrone and dividing by 400 to give area in km^2 units. The option of hourly or quarter hourly isochrones is available, but this could be adapted for any other time period if necessary.

For a typical catchment (for example the Mole at Kinnersley Manor of area 146km^2) the whole process of scaling the catchment and preparing the model input data set requires about 90 cpu seconds.

Isochrones have been derived for all 9 catchments considered in the study based on constant velocities of 0.5m/s and 0.1m/s for river and land paths respectively. The inferred unit hydrographs, maps of relief, slope and the river networks, and histograms of slope frequency within whole basins or individual radar grid squares have also been produced.

DTM's may also be displayed in '3-D' using the Explorer visualisation package on the Silicon Graphics Workstation, allowing the user to 'move around' the catchments on screen.

3.3 Velocity Models

3.3.1 Simple Isochrones

Isochrones may be inferred from the DTM by relating velocities to morphological parameters such as slope and stream length. The simplest approach is to assume time of travel to be directly proportional to stream length such that

$$\tau = \frac{\ell}{v} \qquad (3.3.1)$$

where ℓ is stream length and v is a constant representing velocity. The temporal spacing of the isochrones is taken to correspond to the model time step, which here is taken to be 15 minutes, the same as the data timestep.

Tracer studies of variations in velocity through catchments (Pilgrim 1977, Calkins & Dunne 1970) suggest that average velocity remains fairly constant, or increases slightly in the downstream direction. This is consistent with data reviewed in Leopold et al. (1964) concerning the variation in hydraulic characteristics in channels which show that most rivers increase in velocity (slightly), depth and width in the downstream direction. The effect of a decrease in slope would appear to be more than compensated for by increases in depth and hydraulic radius with increasing distance downstream.

Velocity variations in land flow are harder to quantify than for channel flow due to the different modes of travel taken by water across land, such as surface runoff, interflow and baseflow. Emmet (1978) presents results of laboratory experiments in surface flow which suggest that surface flow, like channel flow, increases in a downslope direction; the effects of slope are compensated for by the retarding effects of friction on higher slopes. As a first approximation the assumption of constant velocity of flow across land would seem reasonable.

Initial work within the present study on the construction of isochrones assumed that time of travel across land and river was directly proportional to the path length, and velocity values were assumed to be 0.5m s^{-1} and 0.1 m s^{-1} for river and land paths respectively. The table below shows the UH time base duration in hours derived from the DTM using these velocities along with those derived from a classical unit hydrograph analysis.

	UH time base, hr	
Catchment	UH derived	DTM derived
Wyre at St Michaels	23	29
Mole at Kinnersley Manor	-	22
Rhondda to Trehafod	18	18

The isochrone maps for these catchments are shown in Figure 3.3.1(a), (b) and (c); isochrones at an hourly time step are shown for the sake of clarity of presentation. Figure 3.3.2 shows an example of the flow paths derived from the DTM used to obtain the isochrones, in this case for a part of the Wyre catchment draining to St Michaels.

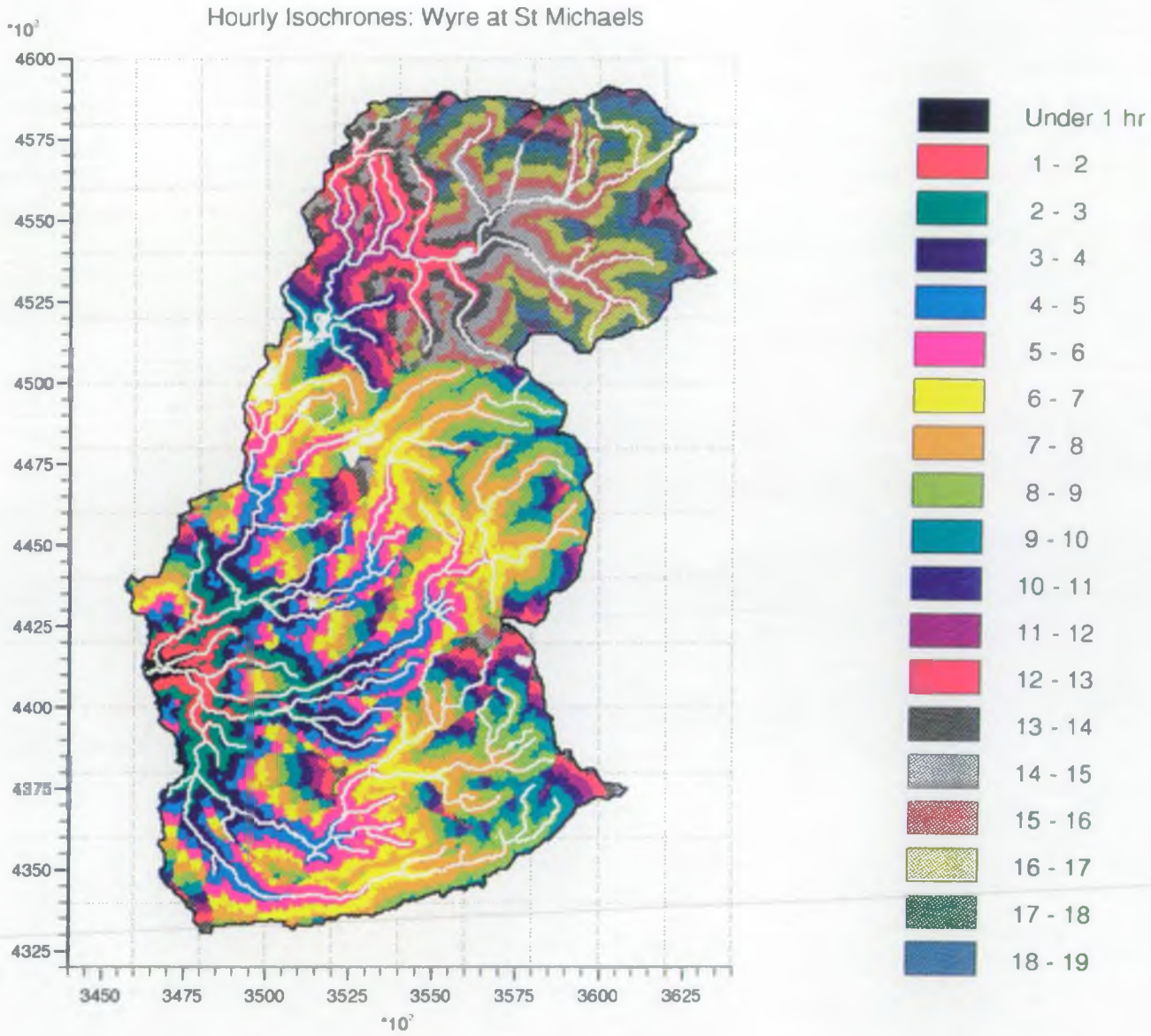

Figure 3.3.1(a) **Isochrone map for the Wyre at St Michaels catchment**

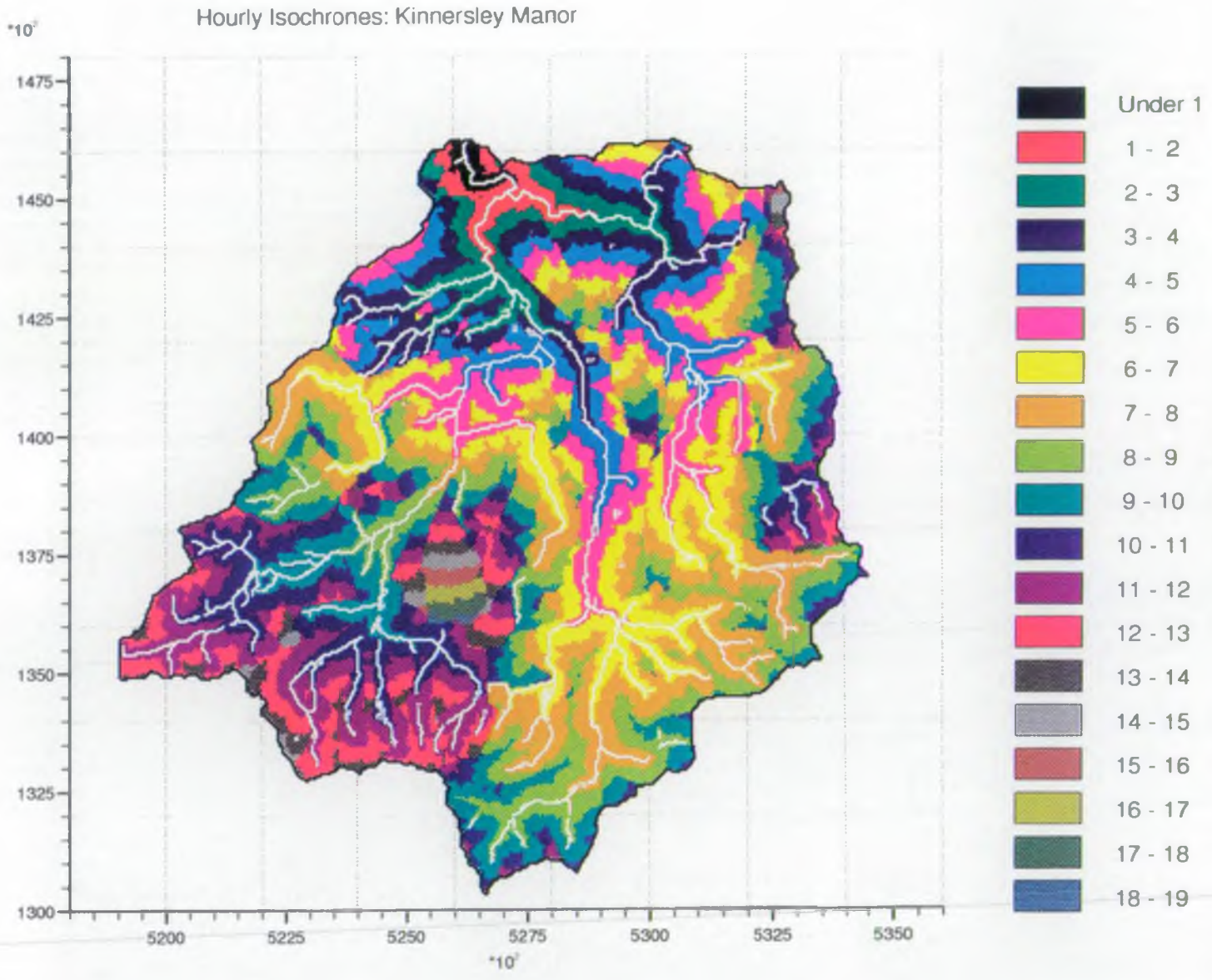

Figure 3.3.1(b) Isochrone map for the Mole at Kinnersley Manor catchment

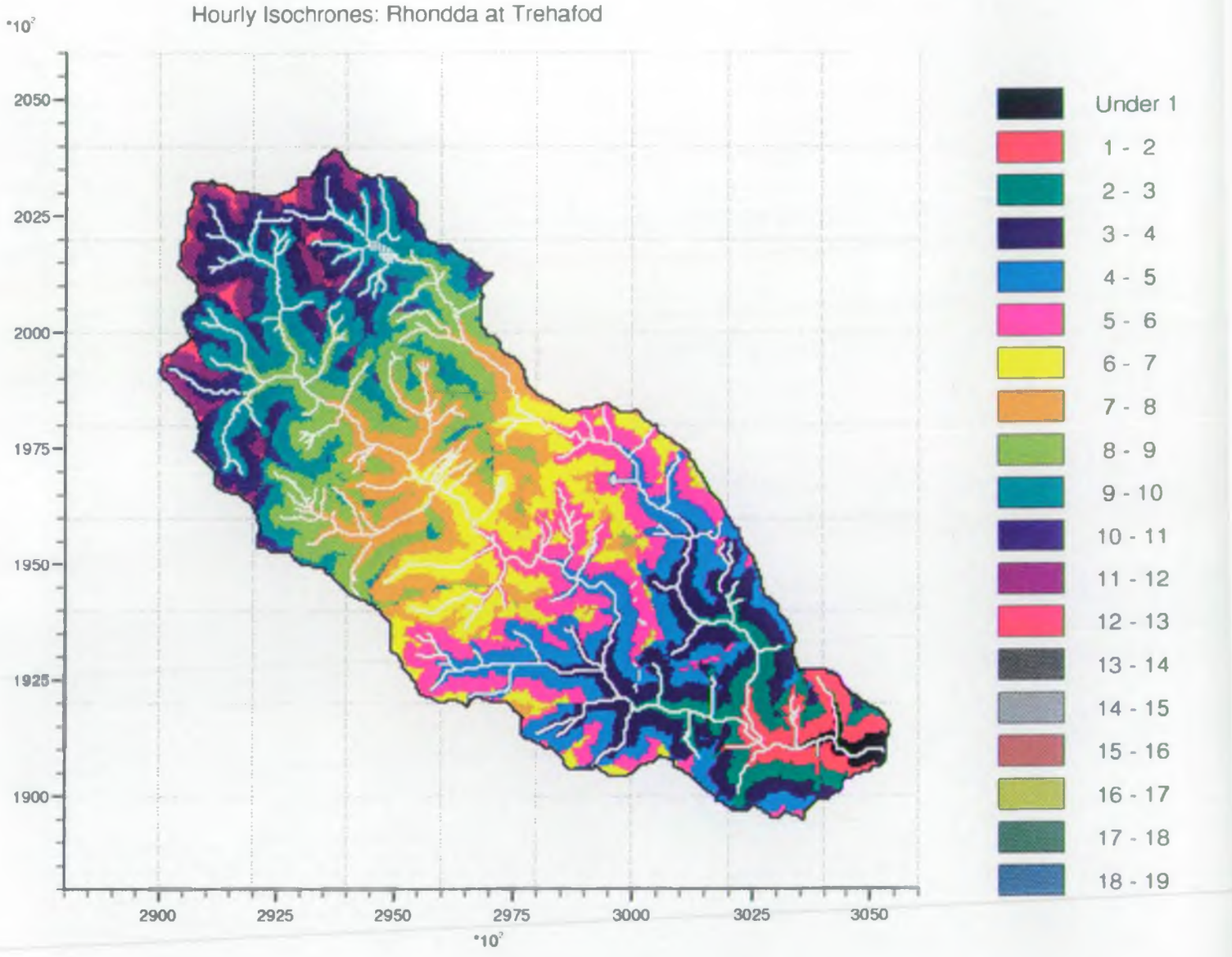

Figure 3.3.1(c) Isochrone map for the Rhondda to Trehafod catchment

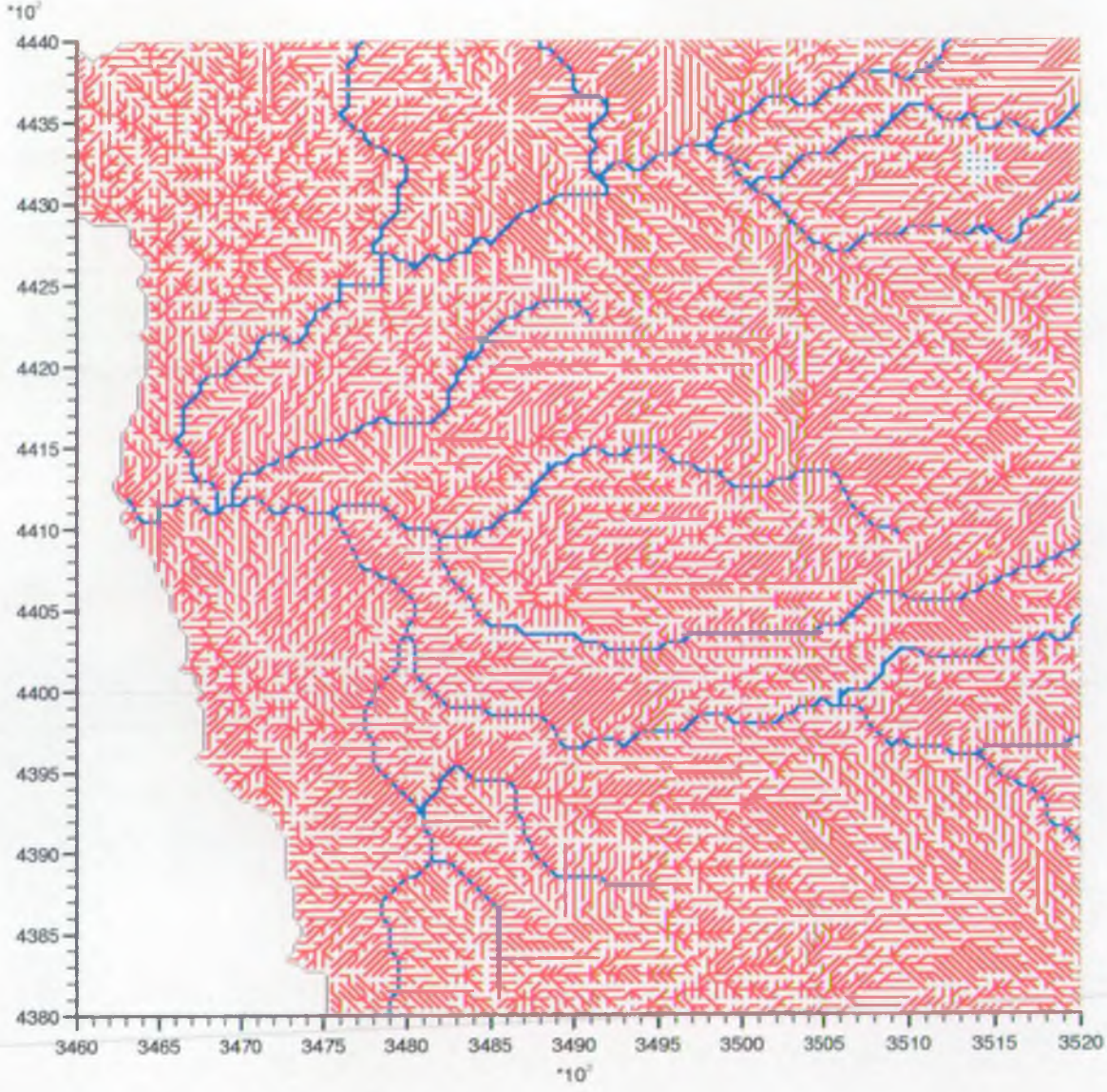

Figure 3.3.2 DTM-derived flow paths for part of the Wyre catchment draining to St Michaels

'Discontinuities' in the isochrones can generally be shown to be due to either natural ridges in the relief highlighting differences in travel time in subcatchments, or to discontinuities in the DTM flow grids. The latter affect mainly the Thames basin catchments. The slope maps in Figures 3.3.3(a), (b) and (c) illustrate the natural ridges in relief seen in all three catchments.

3.3.2 Isochrone Optimisation

A natural extension of the fixed velocity model is to incorporate the determination of the fixed velocity values into the model optimisation framework. The Catchment Definition algorithm has been adapted to produce sufficient information for the model to update the $w_{r,j}$ values based on new velocities every time the model is run. The minimum information for each DTM grid point in the catchment necessary to calculate the new isochrones consists of j, the number of the radar grid square, and ℓ_R and ℓ_L, the distances travelled over river and land to the DTM point. Land and river velocities are regarded as model parameters, with travel times of each grid point to the outlet calculated as previously, using equation (3.2.2).

Initial results suggest the optimisation to be successful in improving the accuracy of model predictions, and calibration generally has the effect of increasing the river velocity and decreasing the land velocity usually giving rise to a longer unit hydrograph base.

3.3.3 Slope Dependent Isochrones

In an attempt to recreate the slight variation of velocity in the downstream direction, travel times dependent on slope have been introduced. The effects of depth and slope on velocity are summarised by the Chezy-Manning equation

$$v = \frac{R^{2/3}\sqrt{s}}{n} \qquad (3.3.2)$$

where v is the velocity, R is the hydraulic radius (related to depth), s is slope and n is the Manning roughness coefficient.

Initial attempts to relate travel time to the slope of the land made the (widely used) assumption that R and n were approximately constant for each catchment. Time of travel from a point in the catchment to the outlet is calculated as

$$\tau = \sum_{i=1}^{N_R} k_1 \frac{\ell_i}{\sqrt{s_i}} + \sum_{i=1}^{N_L} k_2 \frac{\ell_i}{\sqrt{s_i}} \qquad (3.3.3)$$

where N_R and N_L are the number of river and land points respectively and ℓ_i is the ith path length. Here, the slope s_i is the slope of the flow path at that point, as calculated by the Catchment Definition algorithm. The parameters k_1 and k_2 are related to $nR^{-2/3}$ and were estimated for each catchment by optimisation.

The assumption of constant hydraulic radius in the catchment has now been reappraised

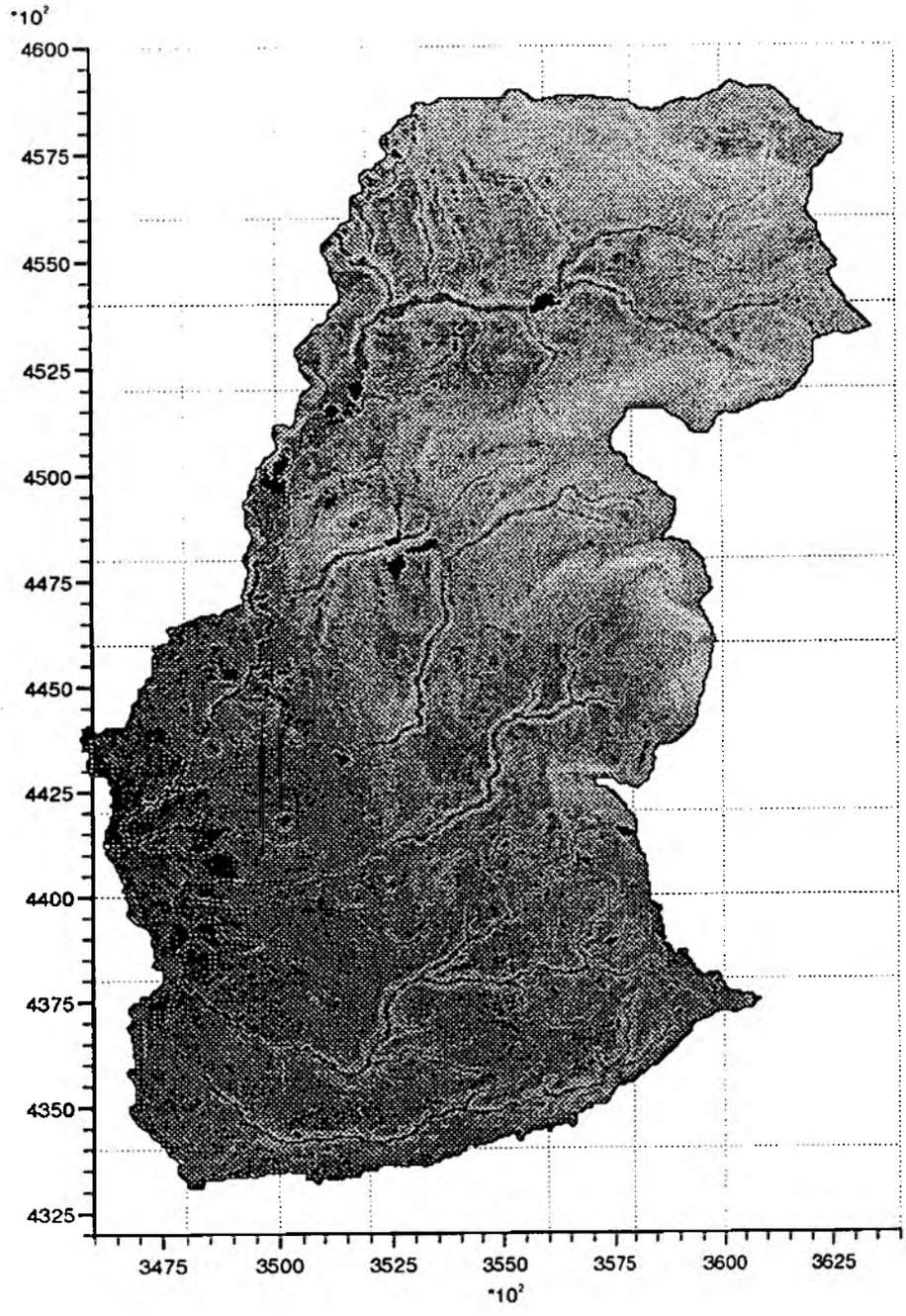

Figure 3.3.3(a) **Slope map for the Wyre at St Michaels catchment**

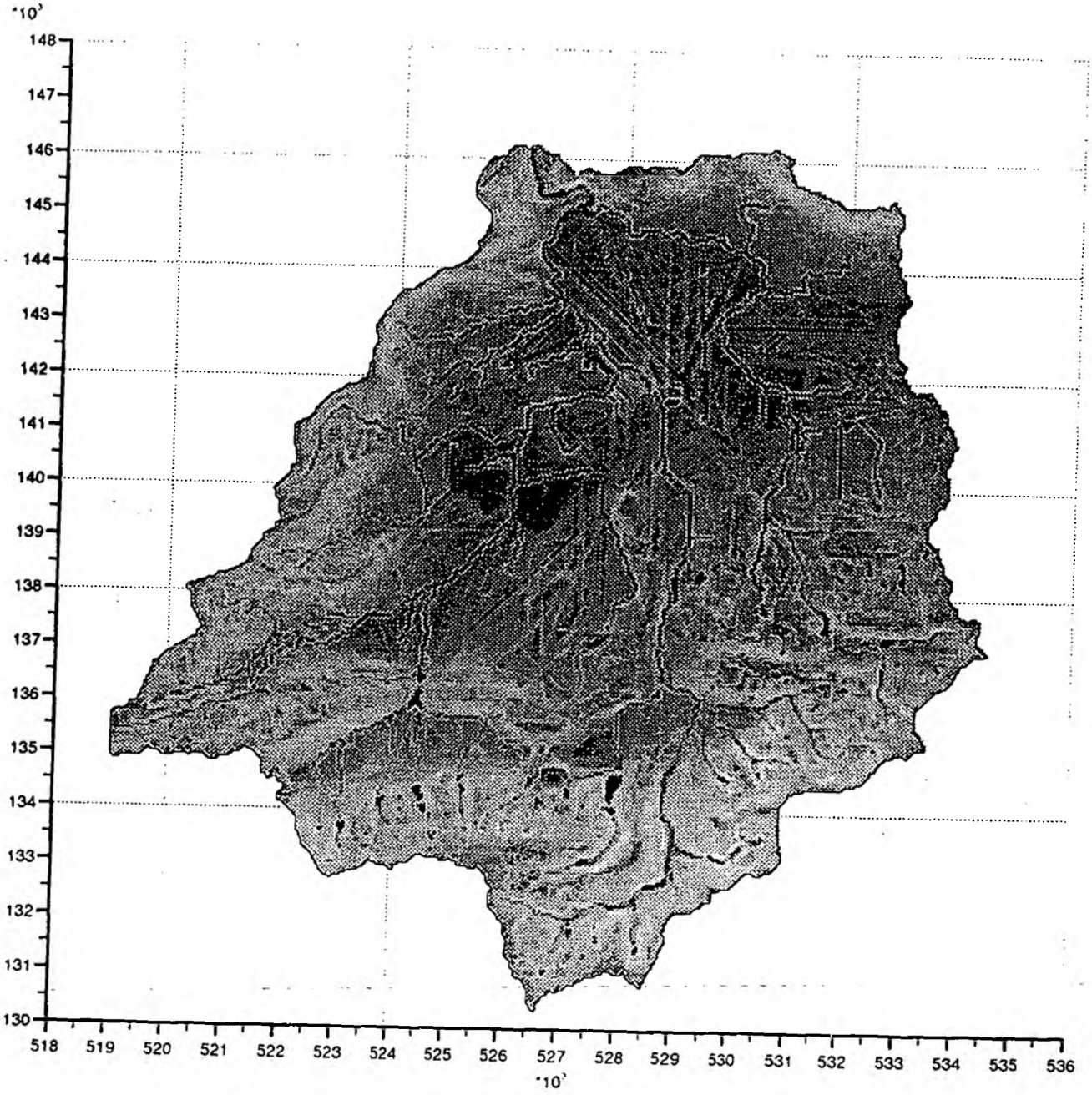

Figure 3.3.3(b) Slope map for the Mole at Kinnersley Manor catchment

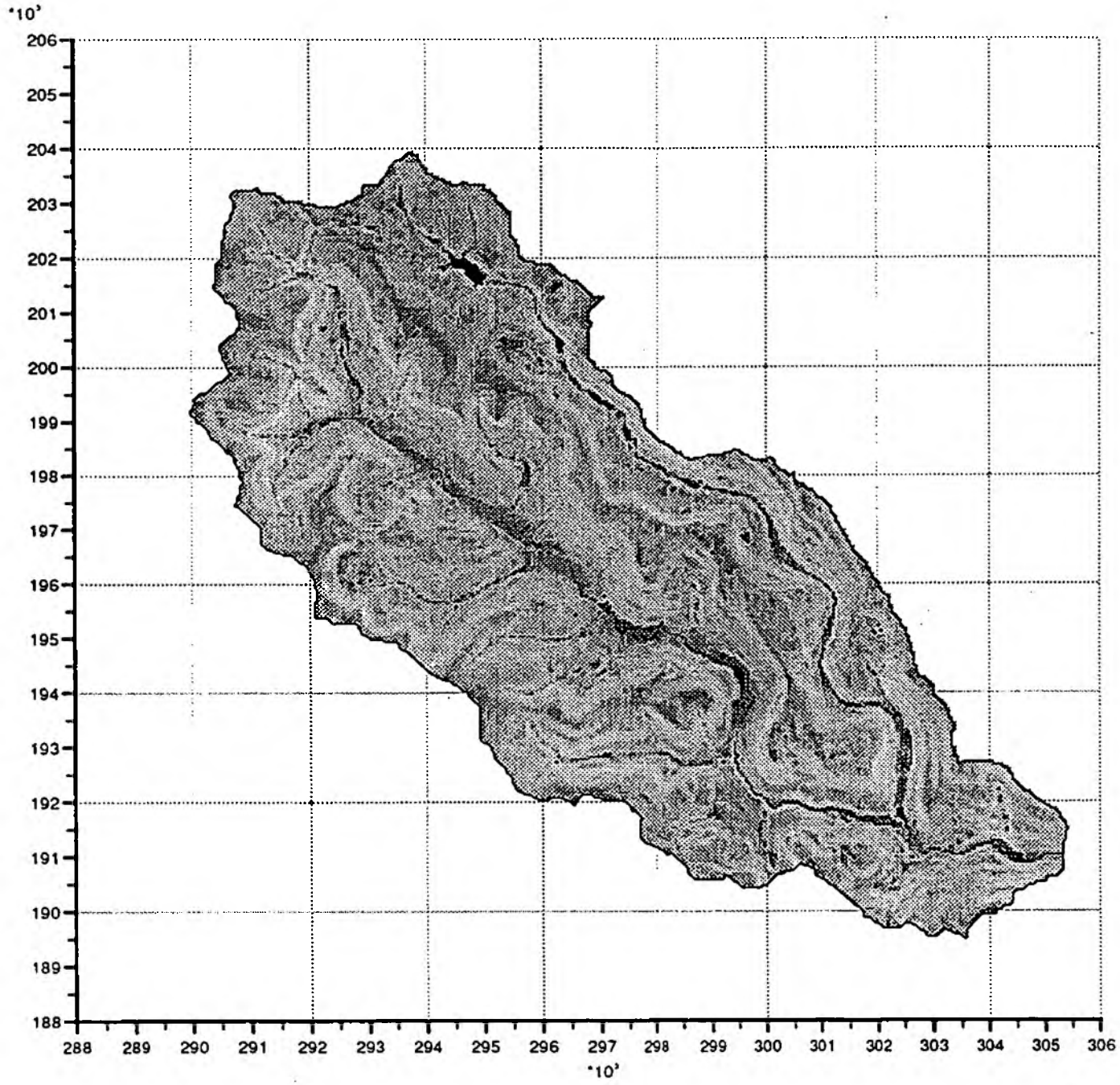

Figure 3.3.3(c) Slope map for the Rhondda to Trehafod catchment

because it leads to a velocity-slope relation of the form

$$v = k\sqrt{s} \tag{3.3.4}$$

resulting in a velocity profile inconsistent with the higher velocities observed in the downstream direction. Pilgrim (1977) notes that this method of calculating travel times in a catchment has often been used, but has never been verified.

Pilgrim tested a number of morphological parameters to control the spacing of isochrones, including the one above and the constant velocity approach outlined in Section 3.3.1. The slope dependent velocity spacing described above was found to be the least accurate estimate for travel times and the spacing of isochrones, and according to Pilgrim "is at variance with all available evidence and should not be used". The assumption of constant velocity was found to provide a simple and fairly accurate estimate of travel times and isochrone spacing, so supporting the method of isochrone derivation in Section 3.3.1.

Isochrone spacing dependent on both slope and hydraulic radius was found by Pilgrim to give the best overall estimates of travel times when the hydraulic radius in each channel was estimated by

$$R \propto L_s^{0.45}. \tag{3.3.5}$$

Here, L_s represents the distance to the point along the stream from its source. This method if isochrone spacing is currently not being used because of the complexity of calculating L_s.The problem stems from the need to know where a DTM river point is in relation to the rest of the river network, which in turn makes the point's distance from source difficult to calculate.

As an intermediate step, an algorithm has been constructed which spaces isochrones according to the Chezy-Manning equation with hydraulic radius estimated by

$$R \propto A^{0.29} \tag{3.3.6}$$

in each channel, where A is the drainage area contributing to the flow in that channel.

From Leopold et al (1964) variation of depth with discharge along a stream is approximated by

$$d \propto Q^{0.38} \tag{3.3.7}$$

and Q is found to vary with drainage area as

$$Q \propto A^{0.75} \tag{3.3.8}$$

which may be combined to give

$$d \propto Q^{0.29}. \tag{3.3.9}$$

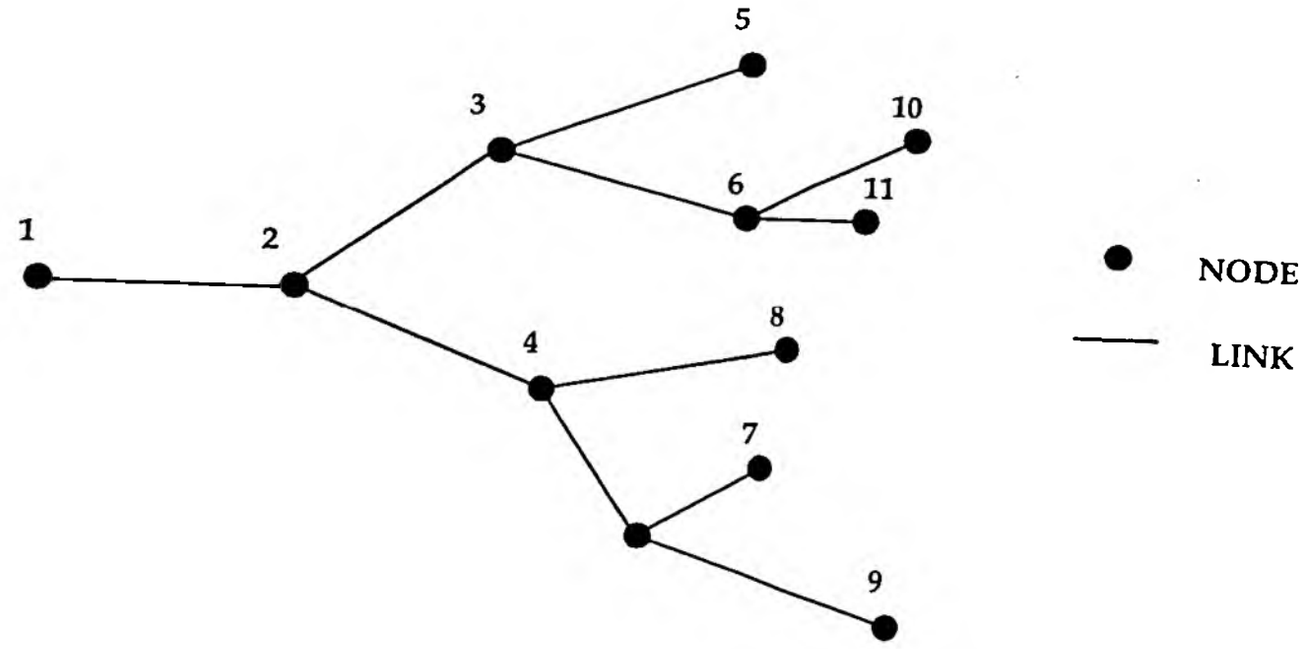

Figure 3.3.4 Numbering of nodes on the river network

These results applicable to 'channels' have been combined with methods used in recent work on river networks (Tarboton et al., 1989) and their construction from DTMs (e.g. Band, 1986). Their approach extracts the spatial structure of river networks and uses it to study the variation of hydrological factors within catchments.

With this aim in mind an algorithm has been constructed which identifies and numbers the different links in a network, establishing where a point on the river is in relation to the rest of the network. As the algorithm climbs the catchment it identifies the branching points (nodes) on the river and numbers them in the order in which it finds them (Figure 3.3.4). As each node is identified, information about each node is stored in the form: elevation, distance along the stream, drainage area and previous node. This information is used to calculate the slope of each link from the relation

$$s = \frac{h}{\ell} \qquad (3.3.10)$$

where h is the fall in elevation at the extremities of the link, and ℓ is the length of the river in the link. The hydraulic radius is calculated from the Chezy-Manning equation (3.3.2). Drainage area contributing to the flow in the link is measured at the downstream end of the link in accordance with Tarboton et al. (1989).

An example, for the Wyre at St Michaels, of the variation of hydraulic radius and slope is shown in Figure 3.3.5. Here the thickness of the river link indicates relative hydraulic radius and the colour of the link gives the relative slope. The figure suggests that calculation of relative slopes and hydraulic radii has been mostly successful, in so far as hydraulic radius

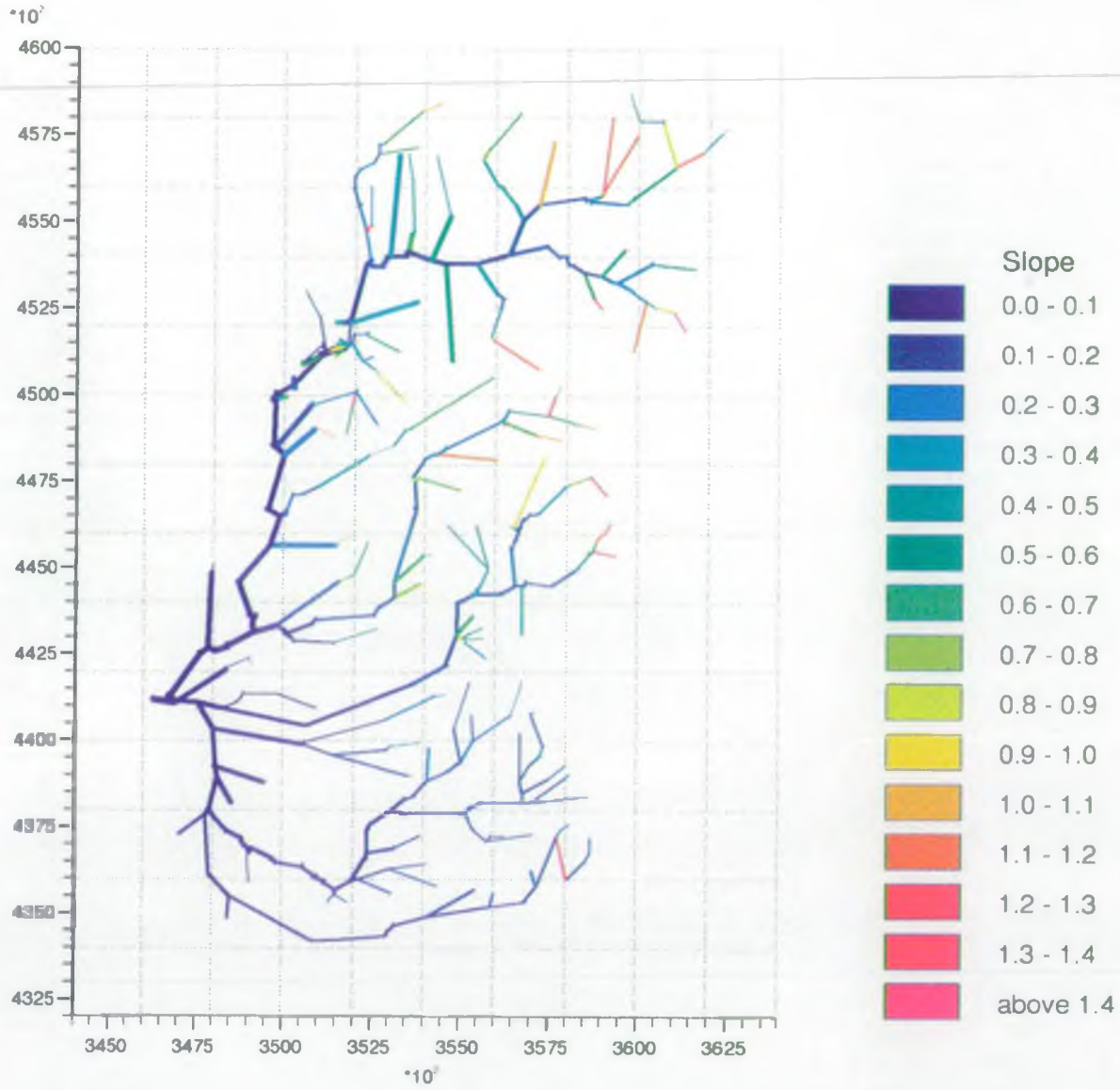

Figure 3.3.5 **River link network for the Wyre at St Michaels: variation of hydraulic radius shown by link thickness and of slope shown by colour scale.**

decreases as slope increases in the upstream direction. The link-derivation algorithm generally performs well in different catchments. However, further work is needed to overcome problems caused by discontinuities in the DTM flow paths in the Thames region, and the difficulties involved in incorporating lakes into the network.

4. LANDSAT-DERIVED LAND USE DATA

4.1 Land classification

The land cover in each study catchment was determined by a supervised classification of Landsat images following the approach described in Roberts *et al.* (1992). These images, comprising seven wavebands from the visible to the thermal part of the electromagnetic spectrum at a ground resolution of 28.5 m, were taken at different dates as follows:-

River Wyre	25th November 1989
River Thames	21st October 1984
Rhondda Valley	22nd July 1984.

The method of analysis was the same for each image:-

(i) Register the image to a 1:50K base map using easily distinguishable ground features.

(ii) Carry out an unsupervised i.e. no additional information, classification of the area of interest.

(iii) Use the statistics from each class identified to provide training areas for a supervised classification of the area of interest.

(iv) Produce the land classification required for modelling purposes - urban areas, agricultural, forestry, open water, and mire areas - by manipulation of the classes obtained. Not all of the above classes would necessarily appear in all of the areas of interest. Also, some parts of the image could not be classified, as in the case for cloud cover in the Rhondda Valley. The agricultural class contains a number of classes - grass, arable and moorland - from the supervised classification.

The results of the image analyses are shown in Figures 4.1 to 4.3. For each area of interest, two figures are shown: a three band (infrared, red and green) colour composite image scales to demonstrate the different land covers, and the resulting land cover classification, colour coded as indicated in the accompanying key. Because the sizes of the areas of interest differed, and were all greater than the area (15 km by 15 km) that could be displayed, the various images were degraded to different extents. The resulting ground resolutions were 60, 150 and 45 m for the Wyre, Thames and Rhondda respectively. This will mean that the visual perception of the three areas of interest will be different. However, this will not be the case when the classifications are used for modelling purposes, as each one has been degraded to give a 50 m ground resolution.

Problems were encountered when analysing each image. For the River Wyre, substantial parts of the image to the north east, shown as the dark areas of the colour composite, were in shadow. These were subsequently classified as moorland/agricultural land, as they were present on the relatively dry steep valley slopes, with no evidence of forestry on the base map. For the River Thames, a small part of the area of interest (the south-west corner) could not be classified, as it was off the edge of the image. Some parts of the Rhondda Valley image was covered in cloud. This could not be re-classified with any degree of certainty.

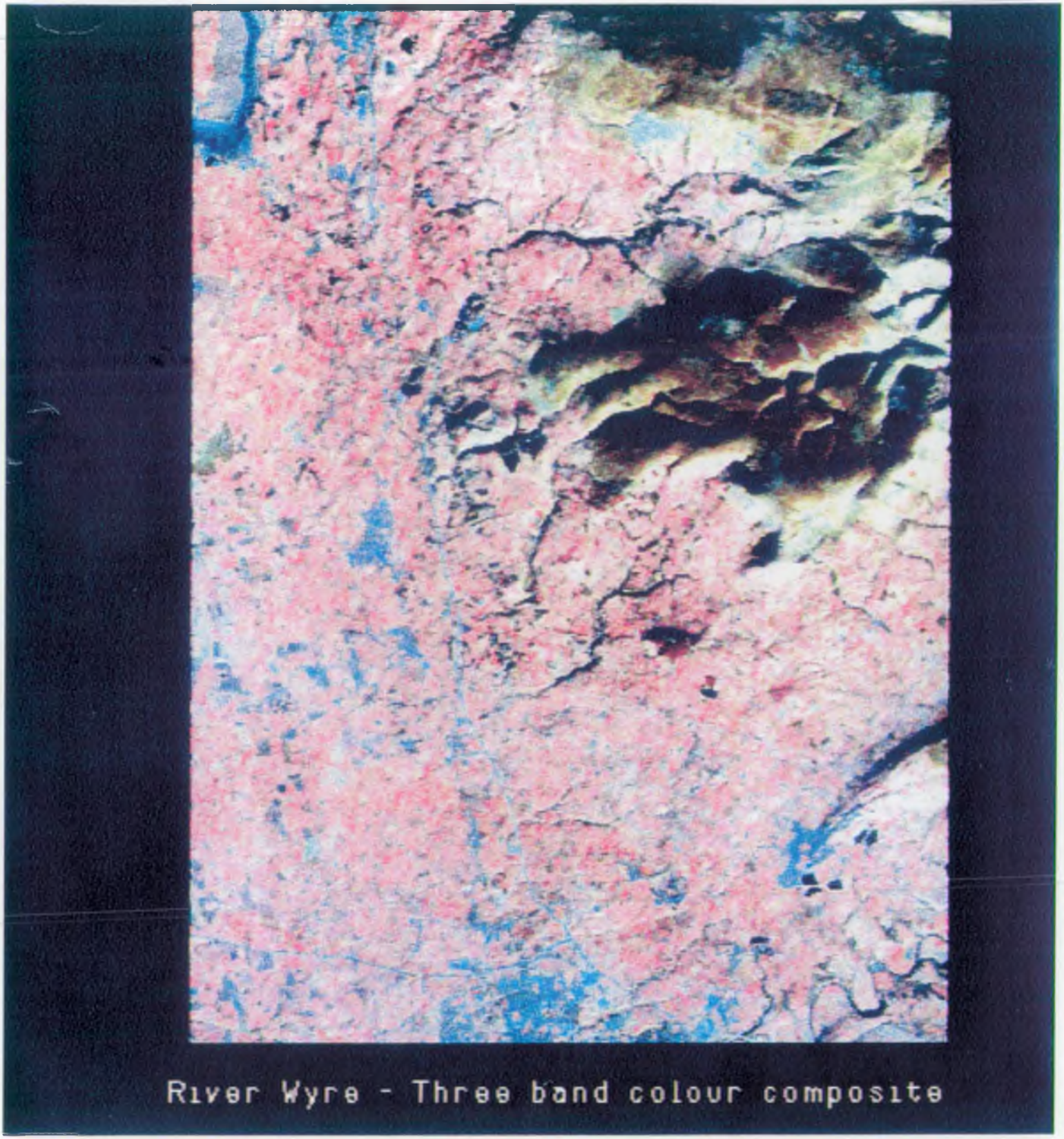

Figure 4.1(a) Three band colour composite Landsat image for the Wyre at St Michaels catchment

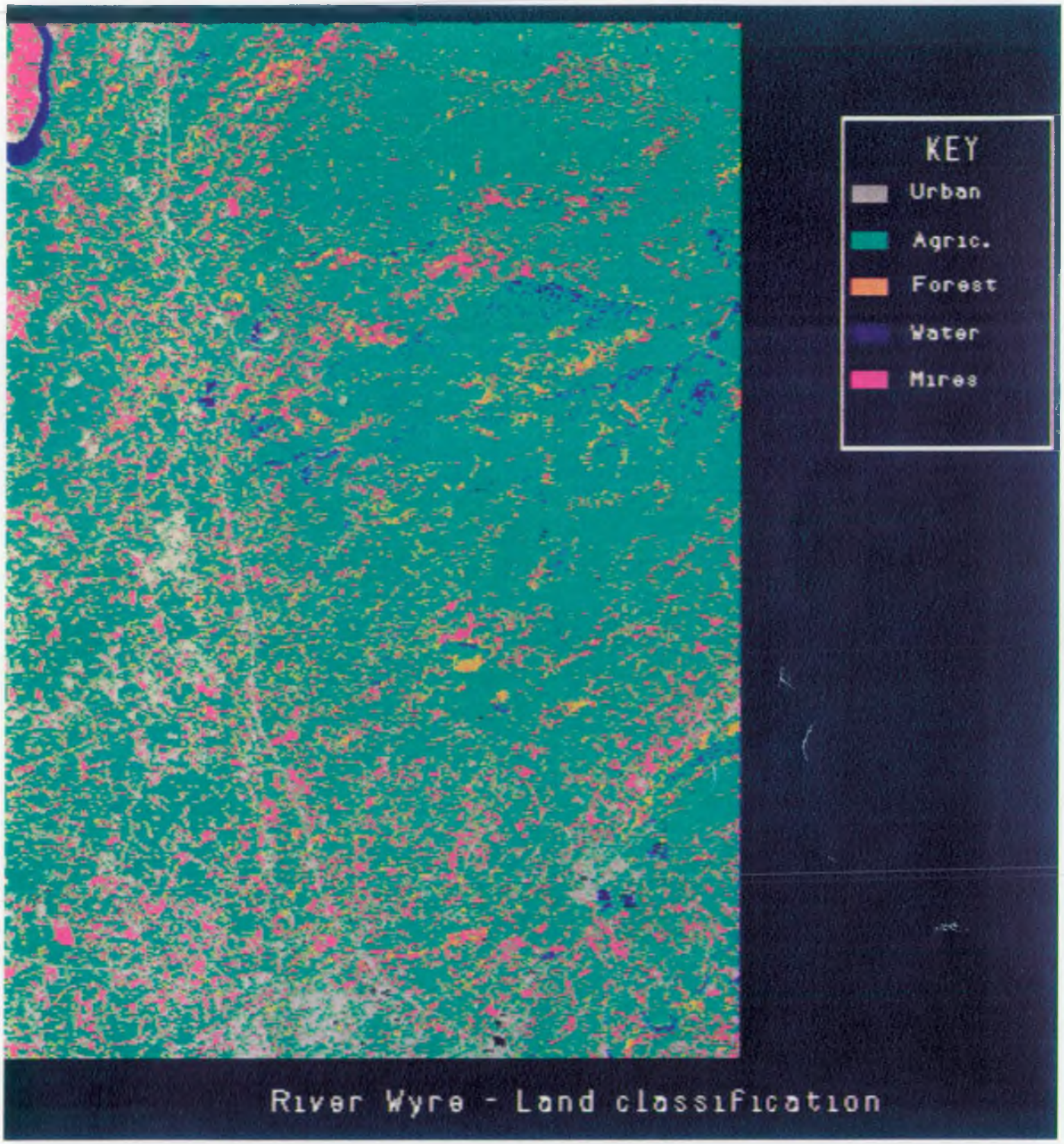

Figure 4.1(b) Land classification Landsat image for the Wyre at St Michaels catchment

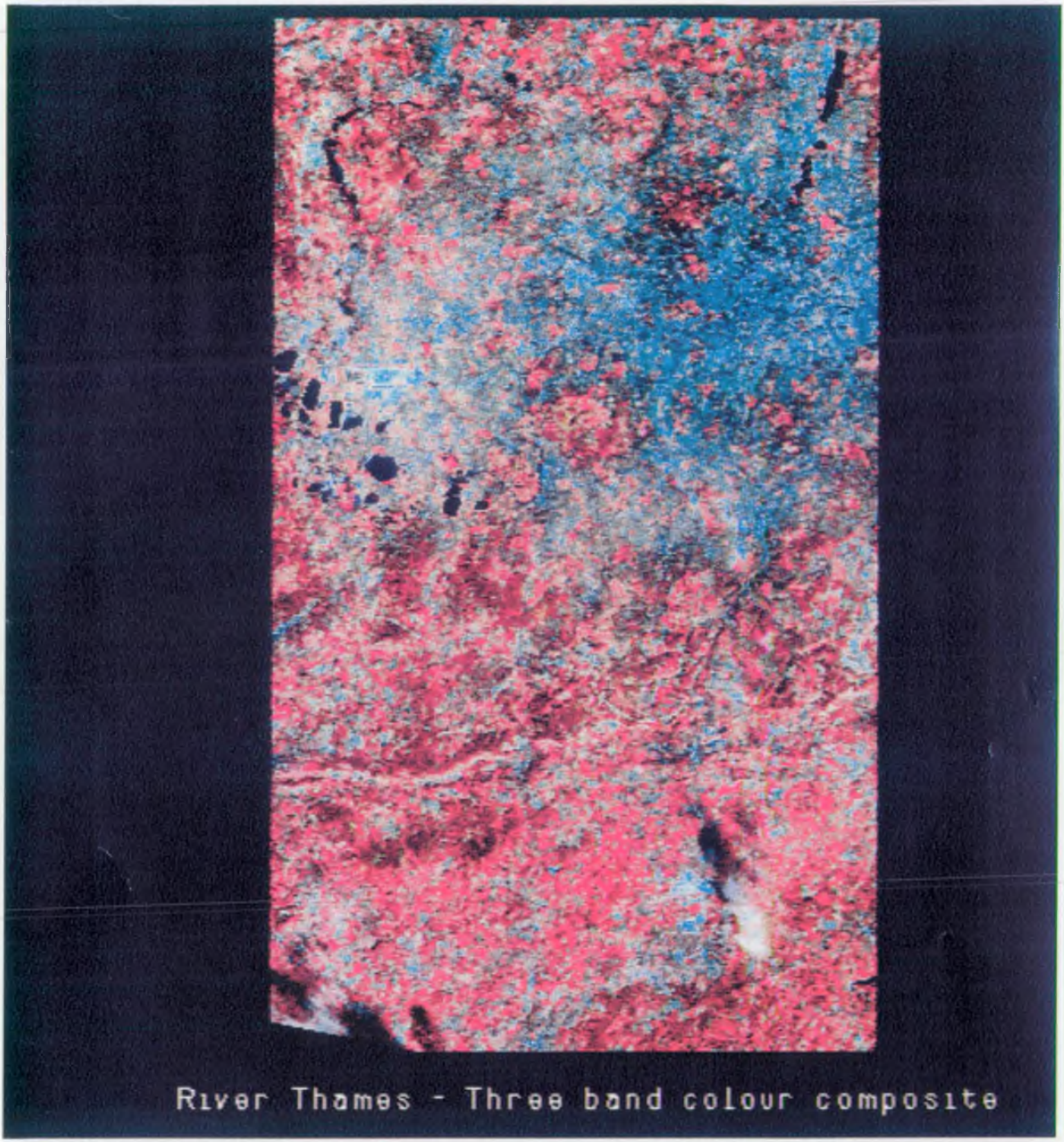

Figure 4.2(a) Three band colour composite Landsat image for the Thames catchments

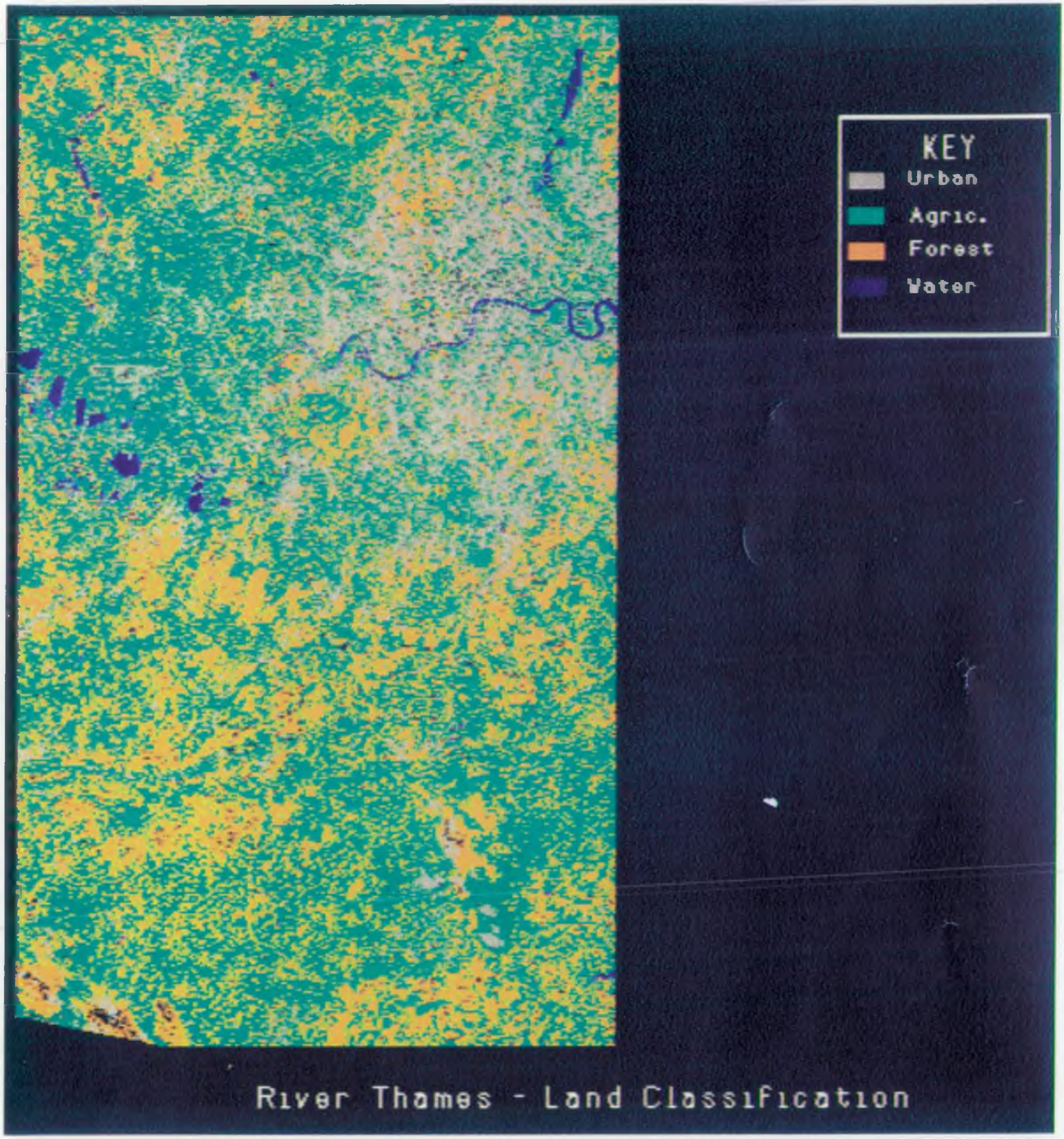

Figure 4.2(b) Land classification Landsat image for the Thames catchments

Figure 4.3(a) Three band colour composite Landsat image for the Rhondda at Trehafod catchment

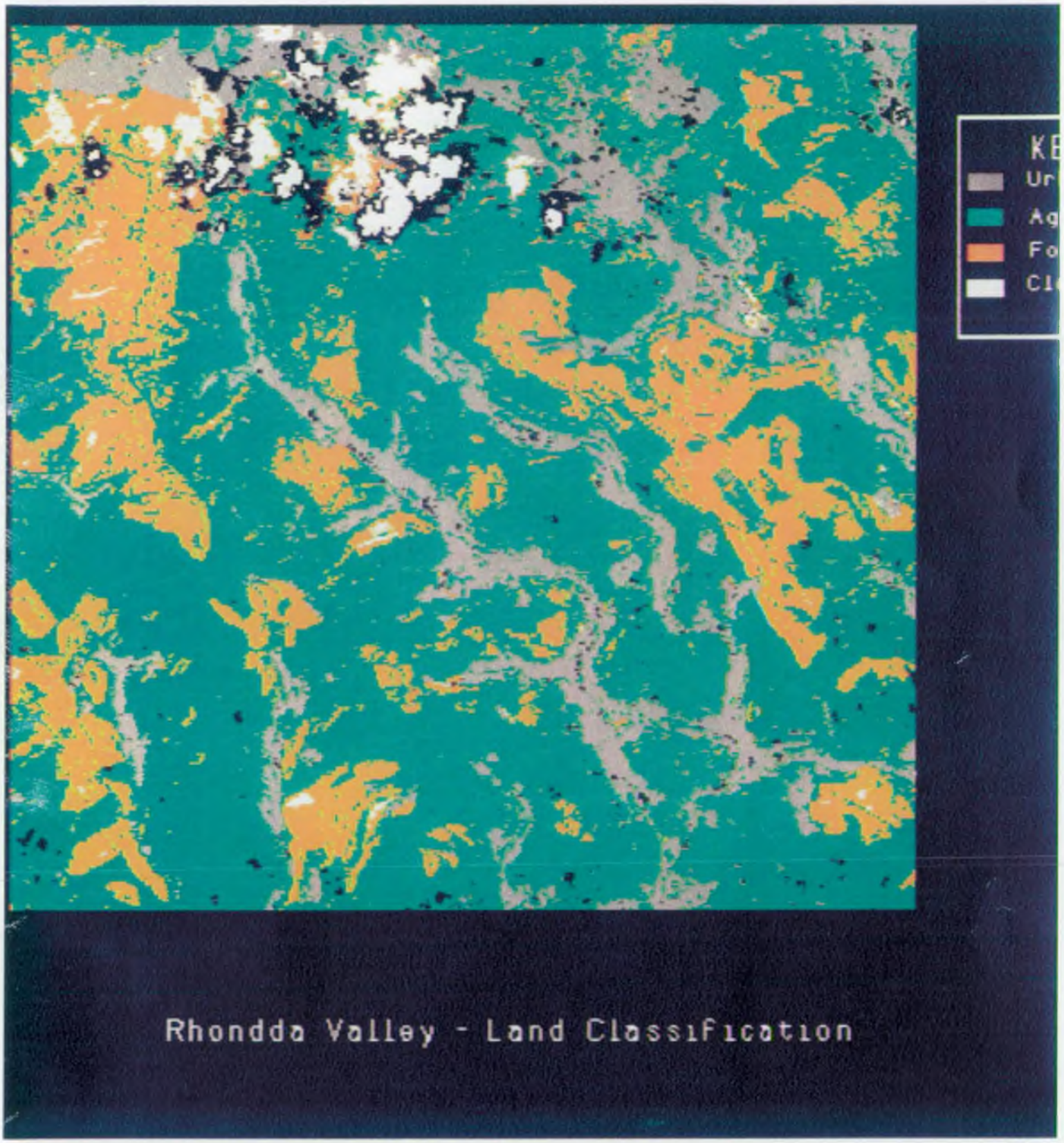

Figure 4.3(b) Land classification Landsat image for the Rhondda at Trehafod catchment

Also, the valley bottoms, classified as urban, are likely to be a combination of land covers - streets, houses, rivers, valley-sides-in-shadow -- and an improved classification of these may be time consuming.

The table below shows the percentages of land cover in each area of interest.

	Wyre	Thames	Rhondda
Urban	6.8	20.3	14.7%
Agricultural	73.2	52.1	62.7%
Forest	2.6	24.5	17.6%
Water	1.1	1.3	-
Mires	16.2	-	-
Cloud	0.1	1.9	5.1%

4.2 Use of the Landsat data in the Model

The 50 m resolution Landsat images are held on the direct access database on the Silicon Graphics Workstations along with the DTM data. This allows them to be accessed by the Catchment Definition algorithm in the same way as the DTM data and be displayed as a 2-dimensional map or superimposed on a relief map. Note that the original classification has been rationalised for modelling purposes, to that at present grass, arable and moorland areas are considered in a single "agricultural" category.

The Landsat data might be incorporated into a distributed model in a number of ways. For instance an evaporation component could be incorporated into the model, that takes into account the dependence of interception loss and evaporation on landuse and vegetation (see, for example, Roberts and Roberts, 1992). The data are currently being included in the model as a simple factor determining storage capacity, with zero storage capacity for urban areas. The Catchment Climbing algorithm has been adapted to produce a grid of values to represent the proportion of each radar grid square that is urbanised. Values are calculated in the same way that grid proportions were calculated before, by keeping a count of the number of DTM grid points classified as urban in each 2km radar square, and dividing by total number of DTM points in each square (1600). These values are then used as input to the model. Initial results are presented later in Section 5.3. Presently 0.7 of the area categorised as urban is taken to have zero storage capacity (i.e. impervious), although there is some experience that a value nearer 0.3 might be more appropriate for Landsat-derived urban areas.

The storage capacity of each radar grid square in the distributed model is currently based on the average slope of the 2km square. The slopes of the four hundred DTM grid points that lie in this radar square are averaged, resulting in a single soil store for the square. Preliminary work has been carried out to assess the value of distributing store capacity within a radar grid square. A procedure has been developed to process the slope data produced by the Catchment Climbing algorithm to produce a data set representing average slopes of four quartiles within each grid square. These may then be used by the model to determine the

depths of soil stores within grid squares.

Slope data for the whole catchment are apportioned into individual grid squares and a (Shell-Metzner) sorting routine used to sort within each grid square in order of size. The quartile limits are slope values and the average of the slopes within these limits are calculated to produce four slope values for each radar square, calculated corresponding to four soil stores for that square of differing capacity.

The model treats these grid boxes in exactly the same way as it does the whole radar squares, allocating each a corresponding store capacity, calculating the runoff generated to the isochrone strips, and translating the runoff to the basin outlet by kinematic wave routing. Results are presented in Section 5 that follows.

Generalisation from 4 to any number of internal slope 'groupings', and consequently more soil stores per grid square, is possible. However, any increase will in turn increase the run time of the model. It should be noted that this approach corresponds to approximating the continuous probability density function (pdf) of slopes over a grid square by a discrete function. An alternative would be to use a parametric form of pdf and develop analytical solutions for the runoff generated from a grid, following the approach of Moore (1985). The result can be very computationally efficient, relative to the discrete approximation approach, depending on the parametric function adopted. However, the simple discrete approximation approach provides a simple initial means of exploring whether a more distributed representation is likely to be of benefit.

5. MODEL EVALUATION

5.1 Catchments for evaluation

Three catchments have been considered for the purposes of model development and evaluation. These are the Wyre at St Michaels in north-west England, the Rhondda at Trehafod in south Wales and the Mole at Kinnersley Manor in the Thames basin; radar rainfall coverage is provided by the radars at Hameldon Hill, Dyfed and Chenies respectively. Details of each catchment are given below along with the radar and raingauge data in current use for model development work. This is followed by a presentation of the initial results obtained from the different forms of model considered so far for two of the three catchments.

Wyre at St Michaels

The Wyre catchment to St Michaels (Station Number: 72002, Grid Reference: 3463 4411) drains an area of 275 km^2 in north-west England. It is almost wholly rural with moorland on limestone, Millstone Grit and Bunter Sandstone. Only one recording raingauge is located within the catchment at Abbeystead Reservoir (Gauge Number: 577804, Grid Reference: 3555 4539) with records back to 1984. The catchment ranges in elevation from 4.4 m at the gauging station, which is slightly affected by tides at low flows, to a maximum of 560 m. Catchment annual average rainfall (for the standard period 1941-70) is 1251 mm. The gauging station is a rated section with a flat-V weir downstream for low flow measurement, the weir being bypassed at high flows. A maximum flow of 164 $m^3 s^{-1}$ is said to have occurred on 11 December 1964 and 1 October, 1967, just below bank full, although the highest gauged flow is 140.5 $m^3 s^{-1}$.

Radar coverage for the catchment is available from the Hameldon Hill radar (Grid Reference: 3815 4289). A total of 92 2 km square radar grids are associated with drainage area to St Michaels gauging station. The model evaluation for this catchment has used radar data for the month of October 1986 along with 15 minute values of rainfall at the Abbeystead gauge and river flow at St Michaels. A simple sine curve with a mean of 1.4 mm day^{-1} has been used as evaporation to support the model water balance calculation. The radar data have been pre-processed to interpolate across areas of anomaly due to blockages in the beam (e.g. a television mast, hills) using the correction method described in Moore *et al.* (1991). Figure 5.1.1(a) shows the anomaly field obtained by calculating the average rainfall rate across all 5 minute radar images over the month of October 1986. Figure 5.1.1(b) shows the anomaly map derived from this average field, demarcating areas for interpolation from adjacent pixel values. Note that the Abbeystead raingauge is situated within the area of anomaly.

Rhondda at Trehafod

The Rhondda at Trehafod (Station Number: 57006, Grid Reference: 3054 1909) drains an area of 100.5 km^2 in south Wales, and is below the confluence of twin valleys: the Rhondda Fach and the Rhondda Fawr. Records from only one recording raingauge at Tyn-y-Waun (Gauge Number: 490291, Grid Reference: 2933 1992) were available to the project. The catchment ranges in elevation from 68.3 m at the gauging station to 600 m and has an annual average rainfall (for the standard period 1941-70) of 2200 mm. Urban areas occupy 13% of the catchment and these are concentrated in the valley bottoms.

(a) Anomaly field

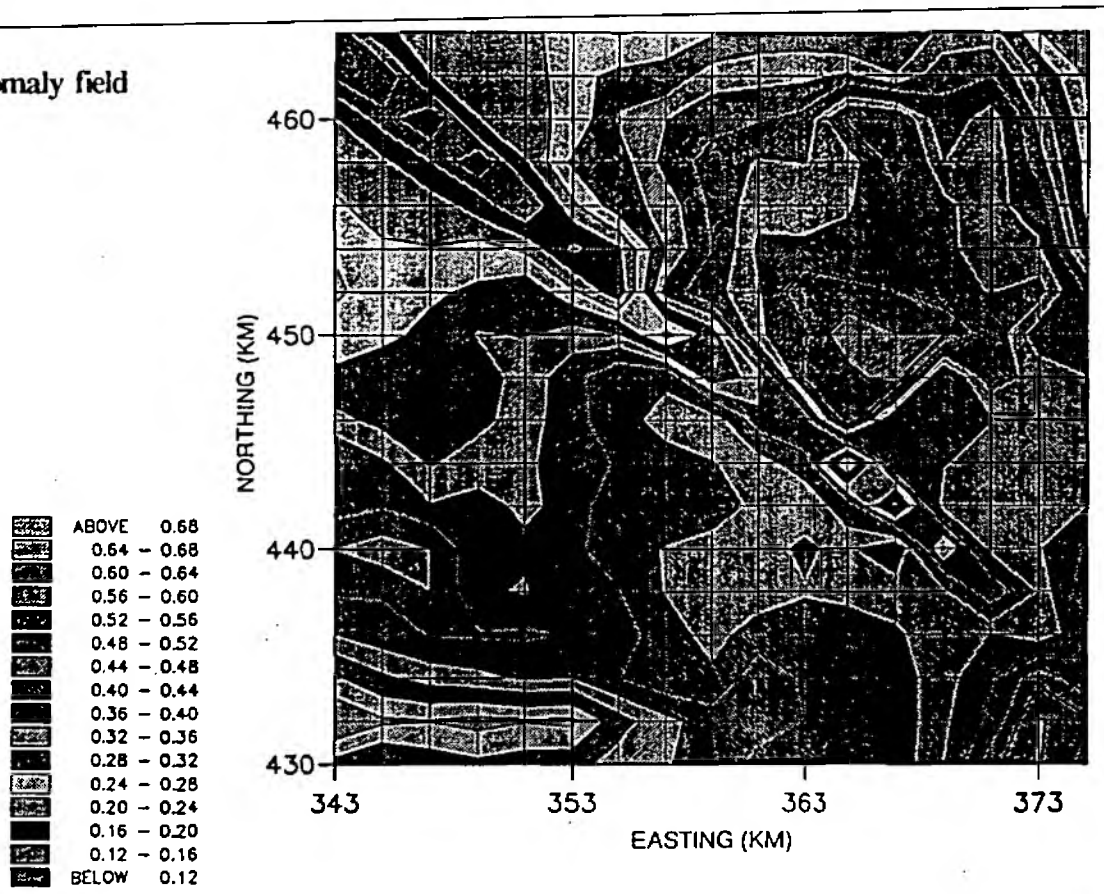

(b) Anomaly map

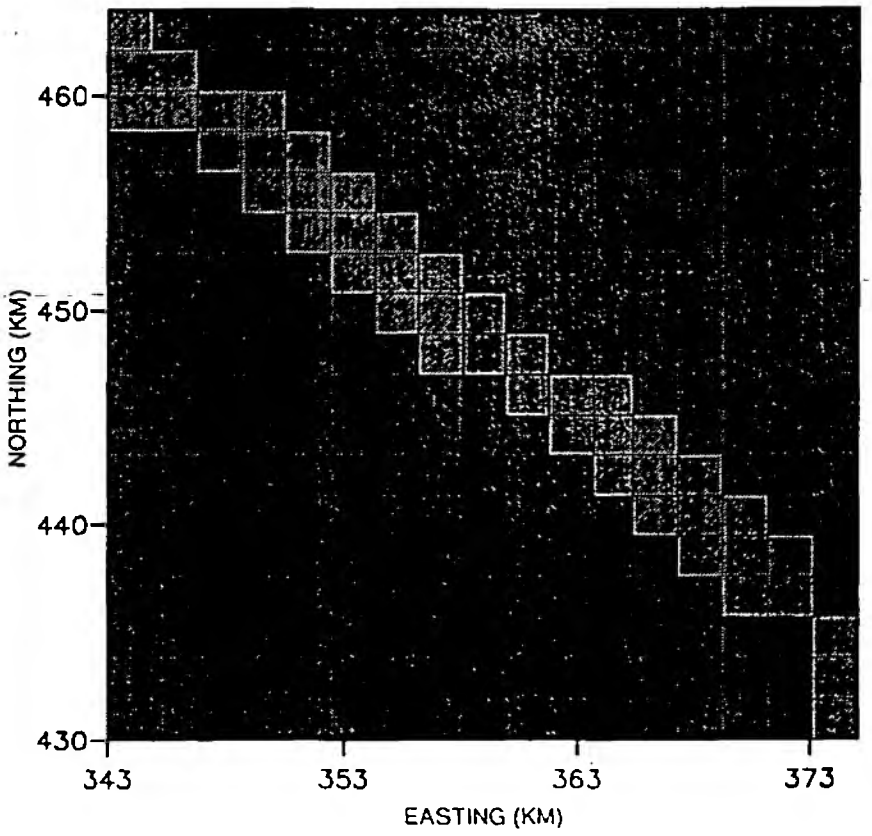

Figure 5.1.1 Correction for anomalies in the 2 km Hameldon Hill radar field for October 1986.

The upper reaches of the Rhondda Fach are controlled by the reservoir at Lluest Wen (capacity: 1073 Ml); Castell Nos reservoir downstream provides very little additional flood storage (capacity: 91 Ml). Gauging is at an engineered river section with a good control, although the recorder intake may be susceptible to blocking by silt from mine wastes.

Radar coverage for the catchment is not ideal with the Dyfed radar at Crug-Y-Gorllwyn (Grid Reference: 2322 2341) being beyond the 75 km "2 km data" range in part. Radar data for the period 1 to 26 February 1990 have been obtained from the Meteorological Office. However, the calibration domain maps for Dyfed have first to be incorporated into IH's software for reading Met. Office radar data off magnetic tapes. Completion of this work is imminent. As a result, the Rhondda to Trehafod has not been included in the model evaluation work reported later in this section.

Mole at Kinnersley Manor

The Mole at Kinnersley Manor (Station Number: 39069, Grid Reference: 5262 1462) drains an area of 142 km^2 to the south of London. It is largely impervious, with largely Weald Clay lithology, supporting a very mixed land use ranging from rural tracts to urban centres (notably Crawley) and the airport at Gatwick. The catchment ranges in elevation from 48 m at the gauging station to a maximum of 178 m and experiences an annual average rainfall (for the period 1972-86) of 806 mm. A recording raingauge is located in the catchment at Burstow (Gauge Number: 284702, Grid Reference: 5306 1437). A rectangular flume with rectangular side sluice has been calibrated by current meter to beyond bankful for flow measurement. Although artificial influences have only a very moderate overall impact on flows, there is a net import of water to the catchment via sewage effluent and some groundwater abstraction.

Radar coverage for the catchment is from the London Weather Radar at Chenies (Grid Reference: 5016 1999) with the "76 km" limit of 2 km data just enclosing the catchment which is associated with 81 2 km radar squares. The catchment is unaffected by anomalies identified in the Chenies radar field. Flow, raingauge and radar data for the period 09.00 22 December 1990 to 09.00 22 January 1991 have been used in the model evaluation work reported here, although additional records are available in IH's modelling database to support further work. A simple sine curve with a mean value of 1.4 mm day^{-1} has been used for potential evaporation in water balance calculations. To support future work on internal and external extrapolation of the model to gauging stations upstream and downstream of Kinnersley Manor flow data are also available in the modelling database for Horley, Castle Mill, Leatherhead and Esher.

5.2 Evaluation Results for the River Mole

The performance of the model, and of its variants, has been evaluated for the River Mole at Kinnersley Manor using both radar and raingauge rainfall data. The model has been calibrated using 15 minute 2km data from Chenies radar and raingauge data from Burstow. A period of one month, from 09.00 22 December 1990 to 09.00 22 January 1991, during which a number of storms occurred has been used for calibration.

Calibration has been carried out on model formulations with increasing levels of complexity, namely:

(i) Model with simple isochrones
(ii) Optimised Isochrones
(iii) Optimised Isochrones + Urban Delineation
(iv) Optimised Isochrones + Distributed Stores Within Grid Squares
(v) Optimised Isochrones + Urban + Distributed Stores

The calibration procedure consisted of inspection and manual adjustment of model parameters followed by automatic optimisation which minimised a chosen objective function. In this case the objective function used was the square of the differences between the calculated and observed flows at each time step.

The results obtained are shown in Table 5.2.1 in terms of the root mean square error (rmse) and the R^2 goodness of fit statistic, the latter indicating the proportion of the variance in the original observations accounted for by the model. A summary of the model parameters and their estimated values for each model type are given in Tables 5.2.2 and 5.2.3. Figure 5.2.1 shows a selection of the results in hydrograph form.

Table 5.2.1 Assessment of different models for the Mole at Kinnersley Manor

Model type	Radar		Raingauge	
	R^2	rmse ($m^3 s^{-1}$)	R^2	rmse ($m^3 s^{-1}$)
Simple isochrones	0.7265	2.76	0.4224	4.02
Optimised isochrones	0.8272	2.197	0.5522	3.53
Optimised isochrones + urban areas	0.8477	2.063	-	-
Optimised isochrones + distributed stores	0.8194	2.246	-	-

Flows predicted using radar data as input to the model are seen to be more accurate than those using gauge data throughout, suggesting that the distributed nature of the radar data improves model performance considerably. The poor performance of the model using raingauge data could however also be due to the gauge's difficulty in measuring high intensity rain accurately; for example the storm in mid January.

As expected, optimising the isochrone velocities on land and river increased accuracy. The automatic calibration had the effect of increasing the river speed from 30 metres/min to 35 metres/min, and decreasing the 'land' velocity from the inferred value of 5 metres/min. The

Table 5.2.2 Model parameter descriptions and units

Symbol	Description of parameter	Units
c	Rainfall calibration factor	-
D*	Soil moisture threshold deficit (or root constant) in evaporation function	mm
S_0	Proportion of soil moisture capacity initially full	-
s*	Regional upper limit of slope	-
S^*_{max}	Regional upper limit of storage capacity	mm
i_{max}	Maximum infiltration rate	mm h^{-1}
α	Storage constant of (cubic) drainage function	hr^{-1} mm^{-2}
θ_r	Wave speed parameter for routing direct runoff	-
θ_b	Wave speed parameter for routing baseflow	-
v_L	Advection velocity of flow along land path	m min^{-1}
v_R	Advection velocity of flow along river path	m min^{-1}

Table 5.2.3 Model parameter estimates for the Mole at Kinnersley Manor (S_0 = 0.8, D* = 75 and S^*_{max} = 75 for all models)

Model type	c	s*	α	θ_r	θ_b	v_L	v_R
Raingauge simple isochrones	.9883	10.25	4.7178×10^{-7}	.7558	.64	5.0	30.0
Raingauge optimal isochrones	.9883	10.25	3.866×10^{-7}	.8957	.6629	1.02	35.01
Radar simple isochrones	1.6778	10.25	6.6817×10^{-7}	.7023	.64	5.0	30.0
Radar optimal isochrones	1.647	10.25	5.7799×10^{-7}	.8631	.5571	1.374	35.01
Radar optimal isochrones urban areas	2.002	10.25	1.4810×10^{-6}	.7997	.4311	1.374	35.01
Radar optimal isochrones distributed stores	2.191	13.75	1.7653×10^{-3}	.6624	.3662	1.374	35.01

(a) Optimised isochrone model, raingauge data

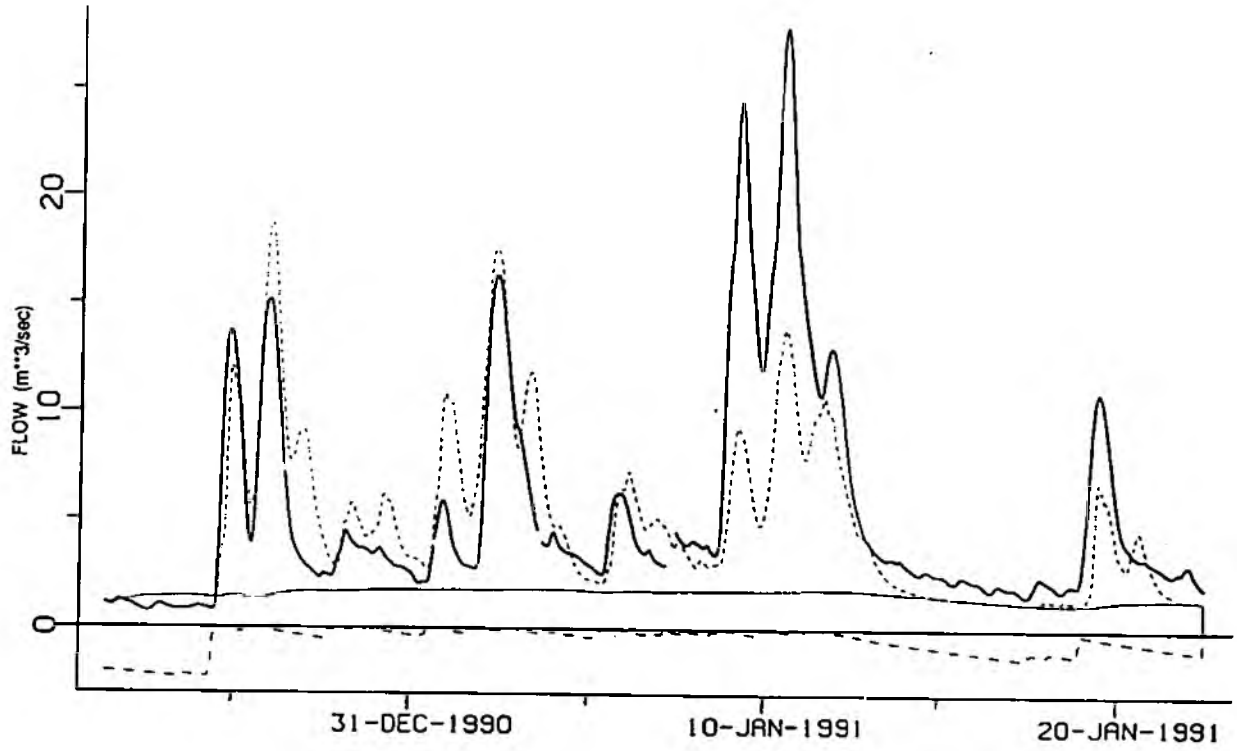

(b) Optimised isochrone model, radar data

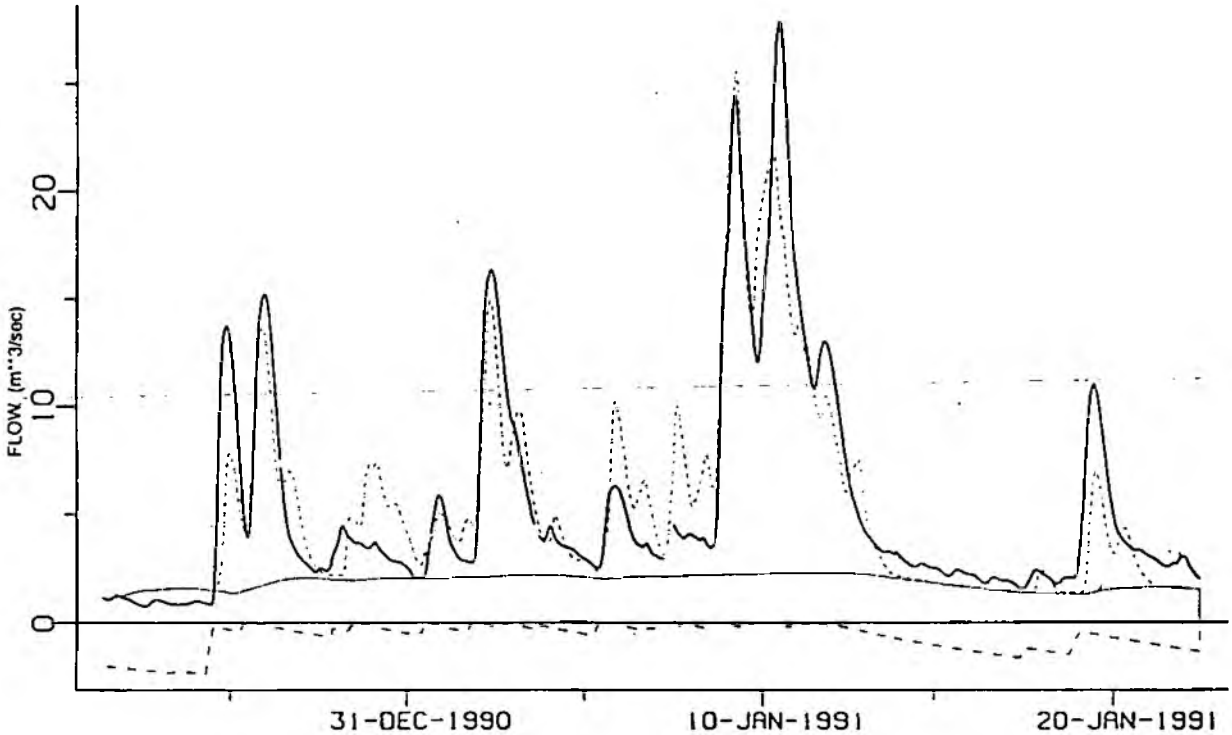

Figure 5.2.1 Model simulation results for the Mole at Kinnersley Manor for the period 22 December 1990 to 22 January 1991 (solid line: observed flow; long dashes: predicted total flow; short dashes: predicted "baseflow"; lower dashed line: soil moisture deficit).

(c) **Optimised isochrone and urban area model, radar data**

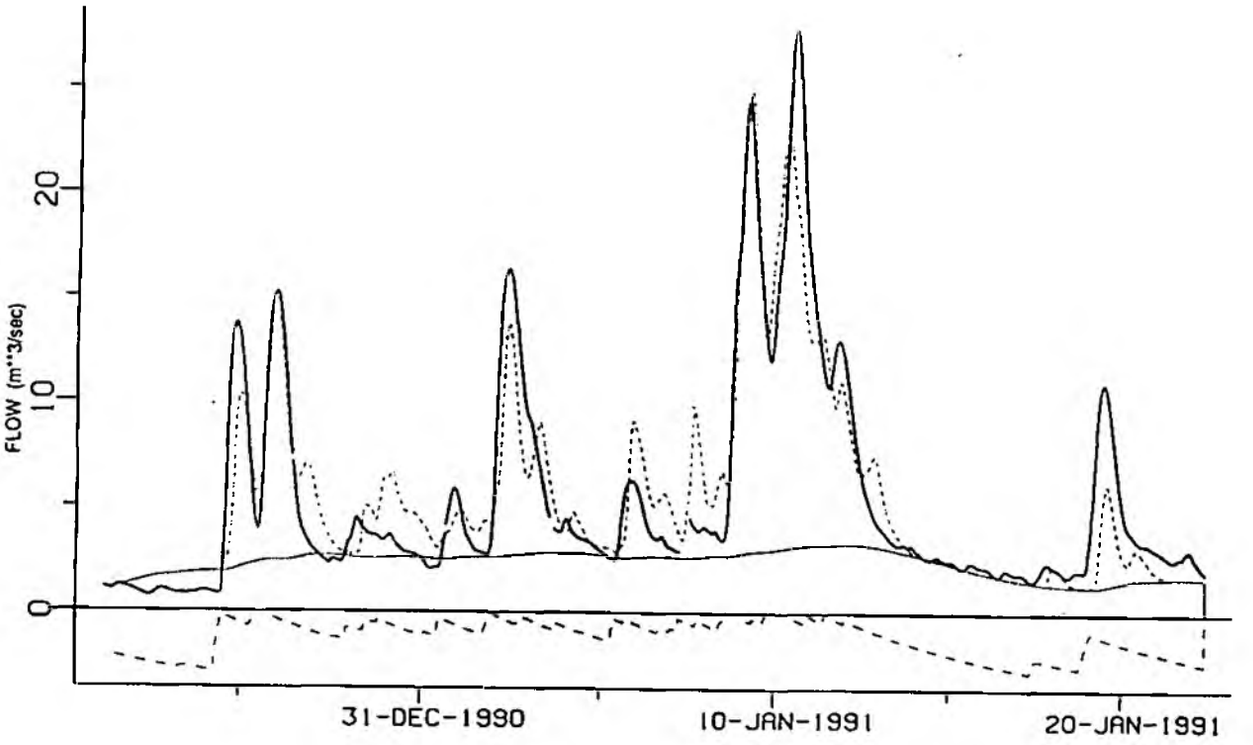

Figure 5.2.1 (cont.) **Model simulation results for the Mole at Kinnersley Manor for the period 22 December 1990 to 22 January 1991.**

effect on the hydrograph base was an increase from 22 hours to over 90 hours, and the optimisation was halted to force the velocities to remain at acceptable values. Those eventually chosen were 35.01 m/min for river and 1.37m/min for land, leading to a hydrograph base of 72 hours. A comparison of the hourly unit hydrographs at the new and old velocities shows that although the time to peak remains roughly the same at around 9 hours, the hydrograph develops a more pronounced secondary peak around thirty hours in the new case and has a relatively long hydrograph base. This is due mainly to the very small 'land' speed resulting in small closely spaced isochrones in regions away from the river, giving rise to a hydrograph with a long narrow tail. The double peak effect in the flow hydrograph after isochrone optimisation is due to the similar shape of the unit hydrograph. "Unit hydrographs" 'before' and 'after' optimisation of isochrones are shown in Figure 5.2.2. Note that these refer to the advective response of the basin to uniform rainfall, and do not incorporate the additional diffusion effect of the discrete kinematic wave scheme used for flow routing. Figure 5.2.3 shows the overall time and space response functions incorporating both advection and diffusion effects for both the slow and fast components of flow. The space response function has its space origin (0) at the basin outlet with positive values increasing upstream and negative values are downstream.

The addition of urban delineation appeared to improve accuracy still further, although the introduction of distributed stores within grid squares made no improvement at all in this case.

(a) Before optimisation: land velocity = 5 m min^{-1}, river velocity = 30 m min^{-1}

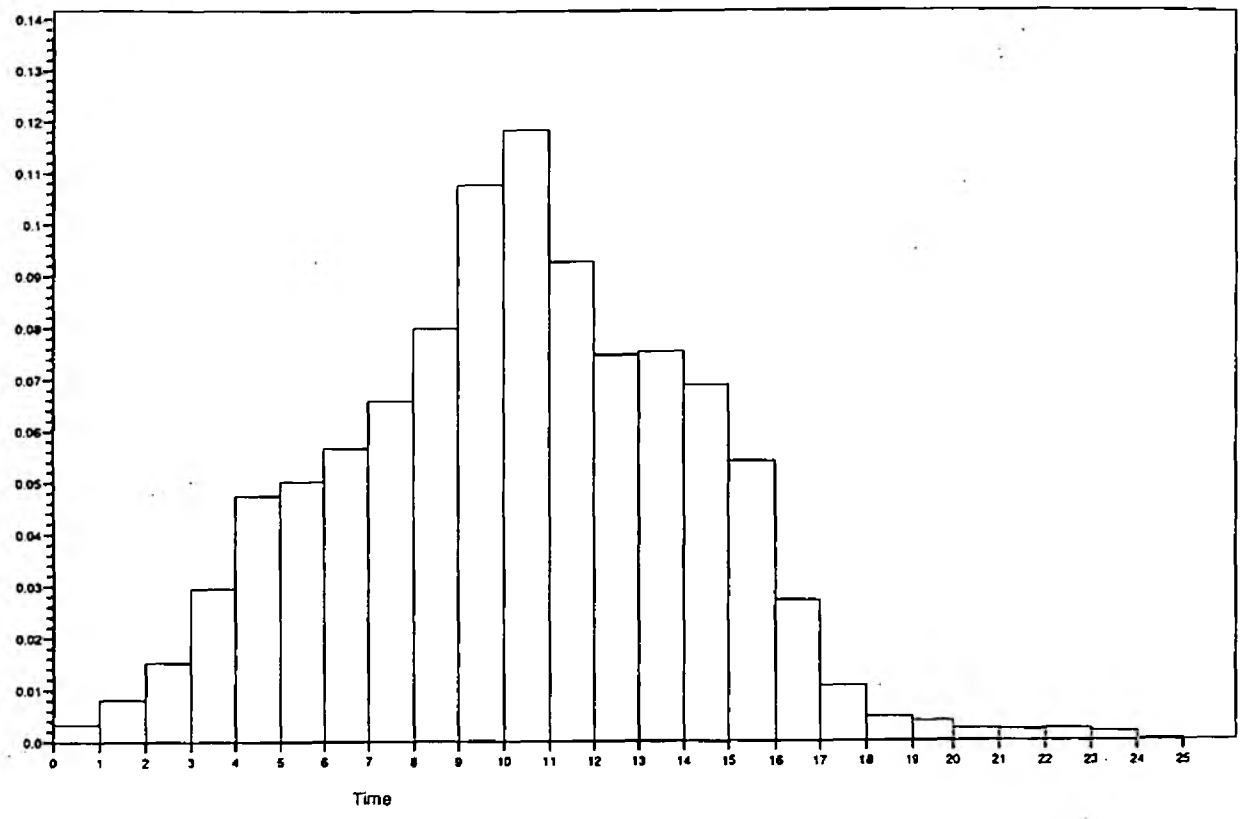

(b) After optimisation: land velocity = 1.374 m min^{-1}, river velocity = 35.01 m min^{-1}

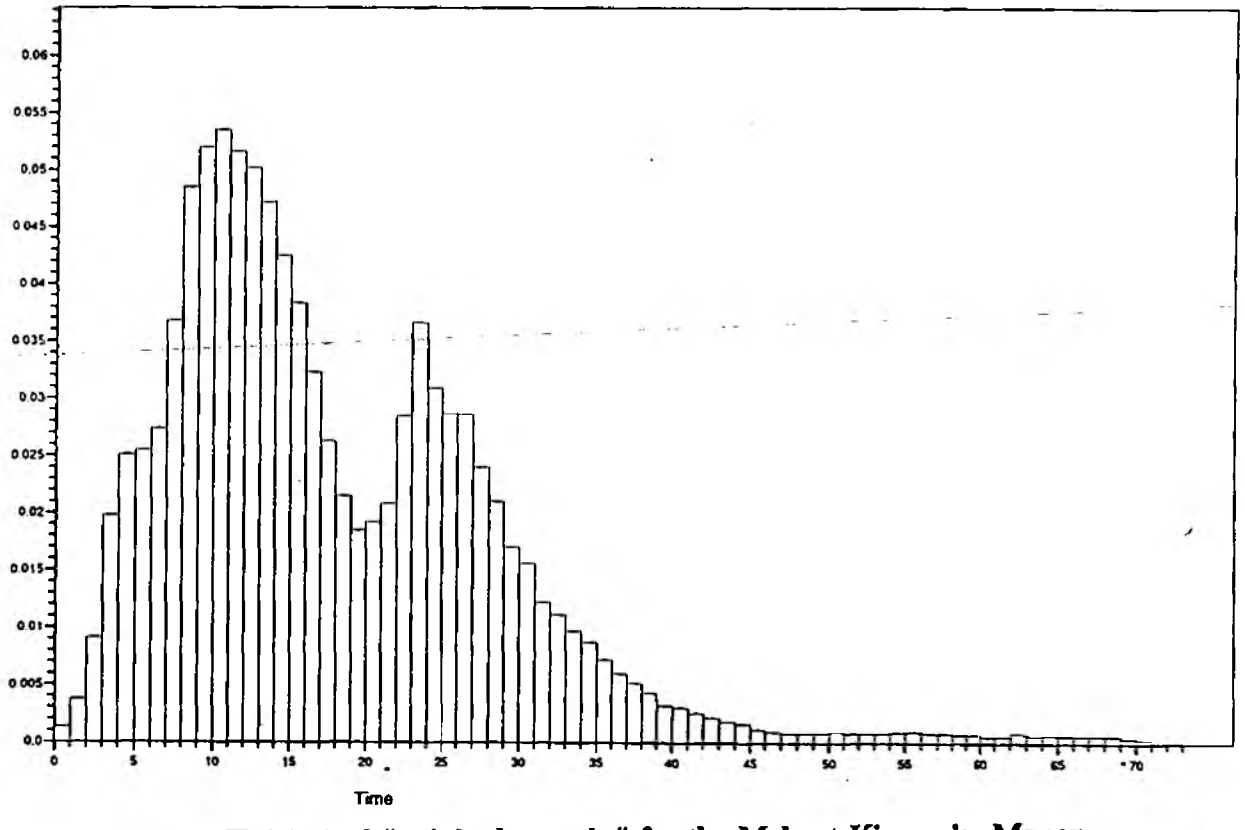

Figure 5.2.2 DTM-derived "unit hydrographs" for the Mole at Kinnersley Manor.

(a) Time response function

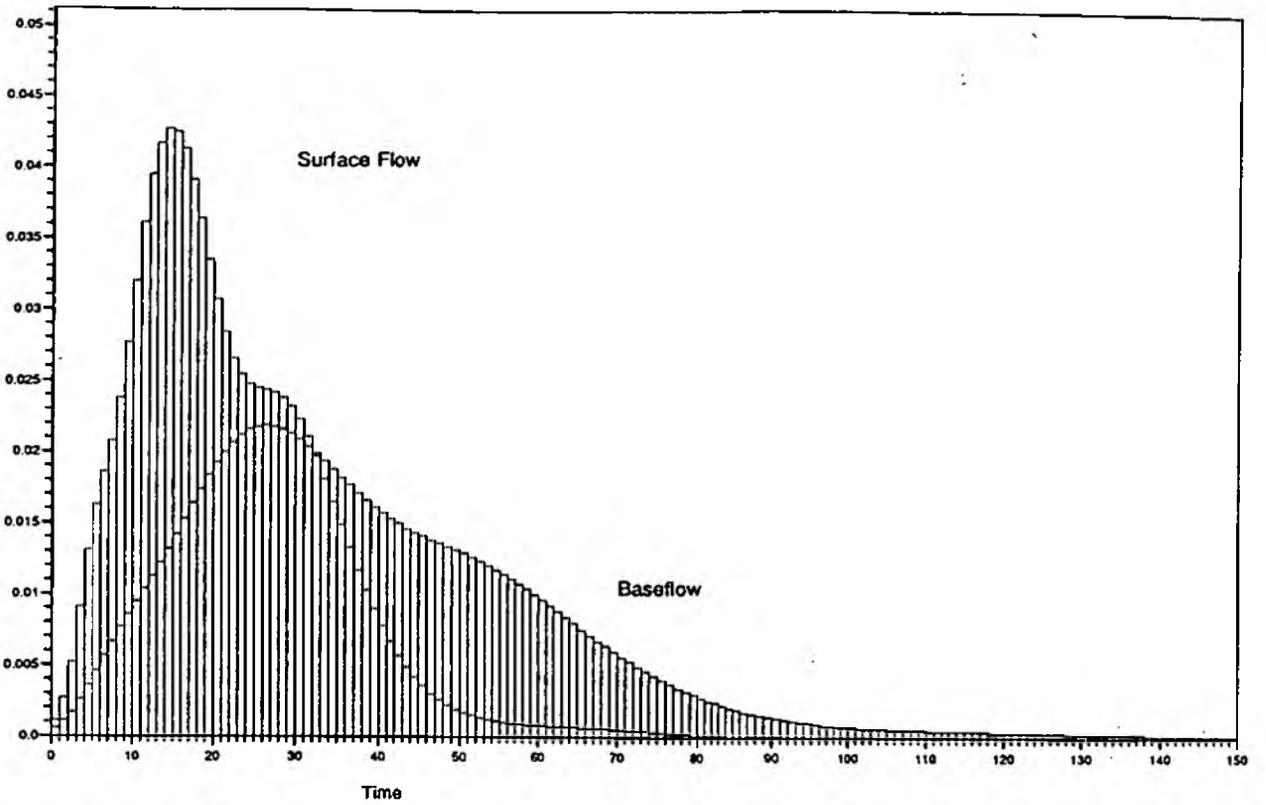

(b) Space response function (fast response only for times 0, 20, 40, 60, 80, 100 hr)

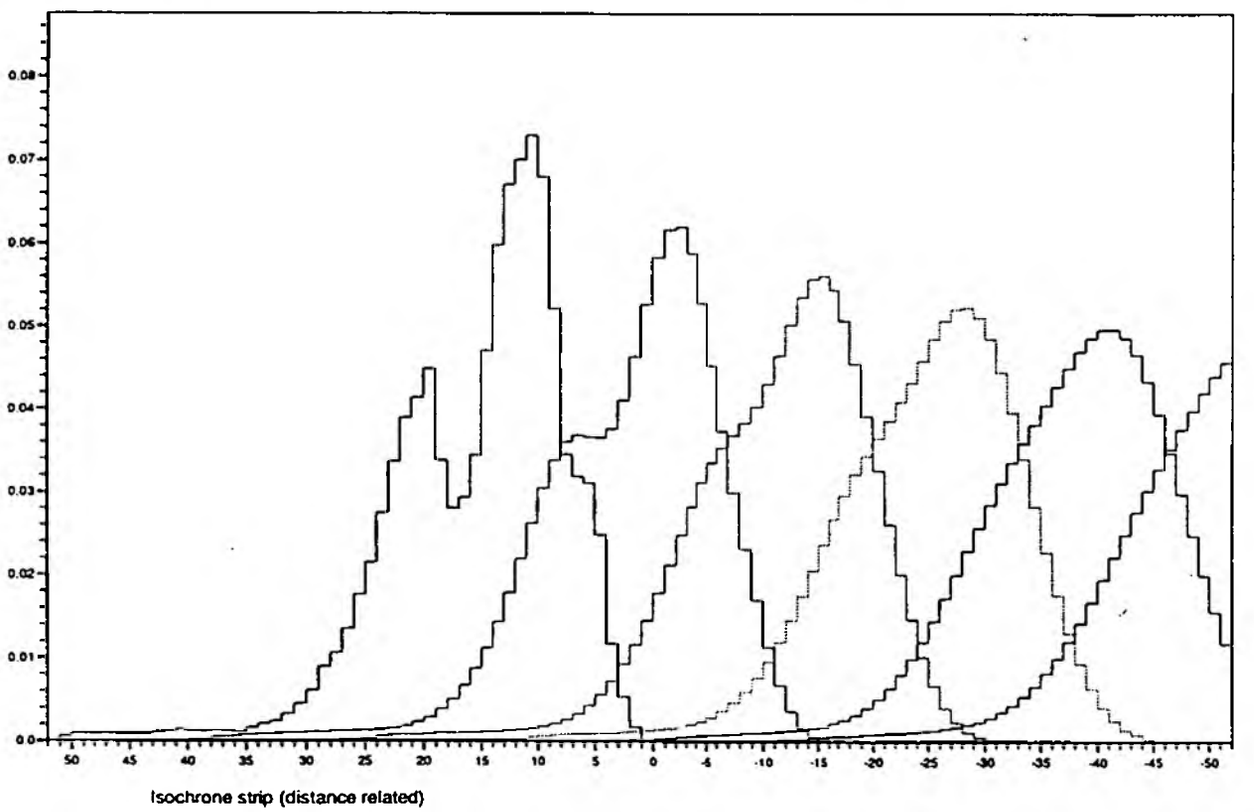

Figure 5.2.3 Model time and space response functions, incorporating time area ("unit hydrograph") and kinematic wave effects, for the Mole at Kinnersley Manor; hourly time step.

With only one month of data, however, it would be hard to generalise at this stage, and further work needs to be done in applying the model to further events.

5.3 Evaluation results for the River Wyre

The Wyre at St. Michaels provides a contrasting catchment to the Mole for evaluation purposes, being located in an upland, hilly region of North West England. Again a monthly period of data, from 0900 23 October to 22 November 1986, has been used for calibration and evaluation purposes. In this case Hameldon 2 km radar data and Abbeystead Reservoir raingauge data are used as rainfall estimates. Table 5.3.1 shows the results obtained in terms of the R^2 and the root mean square error performance criteria. Table 5.3.2 presents the parameter estimates obtained for each variant of the model. Figure 5.3.1 shows the observed

Table 5.3.1 Assessment of different models for the Wyre at St Michaels.

Model type	Radar		Raingauge	
	R^2	rmse ($m^3 s^{-1}$)	R^2	rmse ($m^3 s^{-1}$)
Simple isochrones	0.6244	11.3700	0.5523	12.41
Optimised isochrones	0.7159	9.8887	0.6788*	10.51
Optimised isochrones + slope distribution	0.6781	10.5272	0.7138*	9.9253*

* Indicates calibration halted to keep values within acceptable limits

Table 5.3.2 Model parameter estimates for the Wyre at St Michaels (S_0 = 1.0, D* = 75 and S^*_{max} = 75 for all models)

Model type	c	s*	α	θ_r	θ_b	v_L	v_R
Raingauge simple isochrones	.6917	24	6.76×10^{-7}	0.9998	0.9600	5.0	30.0
Raingauge optimal isochrones	.8016	24	9.76×10^{-7}	0.9600	0.7195	4.348	47.068
Raingauge distributed stores	.8006	25.71	$2.1164\ 10^{-7}$	0.9068	0.7195	4.348	47.068
Radar simple isochrones	.6694	24	8.3061×10^{-7}	0.9998	0.5691	5.0	30.0
Radar optimal isochrones	.6656	24	8.1106×10^{-7}	0.9998	0.5691	3.215	42.69
Radar distributed stores	.6890	31.37	3.8121×10^{-7}	0.9998	0.5691	2.778	42.577

(a) Optimised isochrone, raingauge data

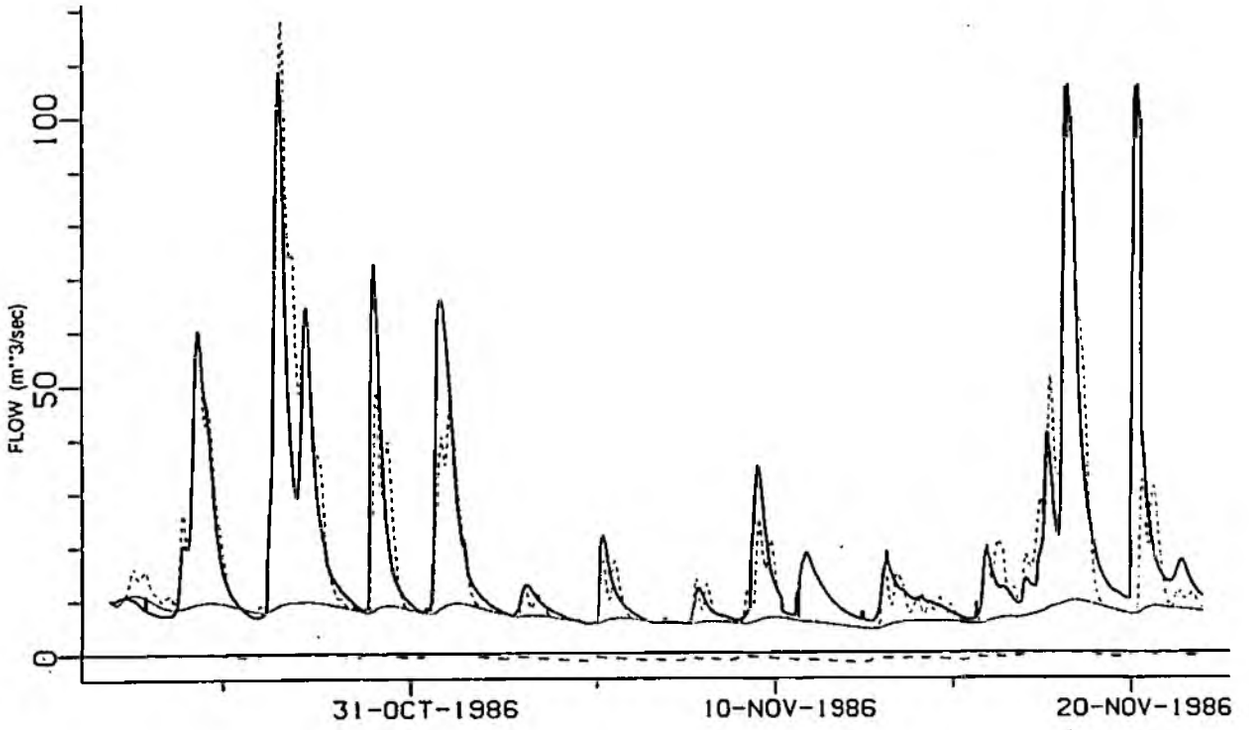

(b) Optimised isochrone, radar data

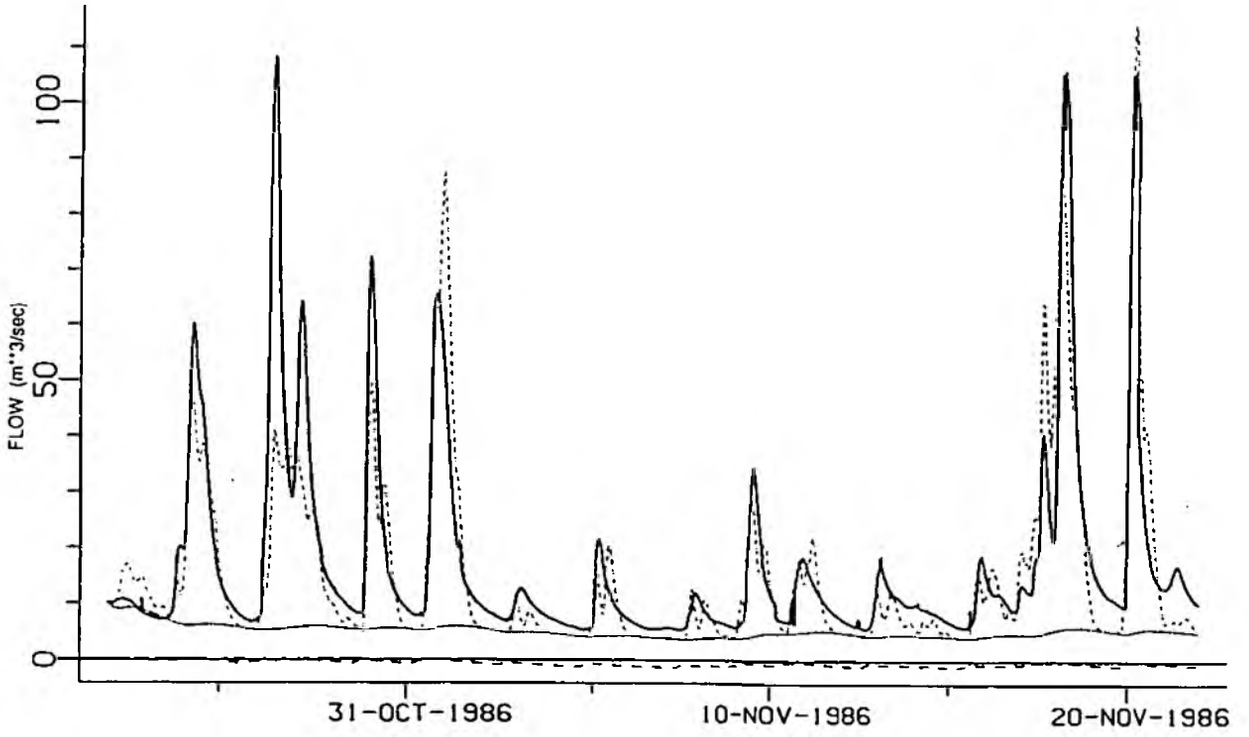

Figure 5.3.1 Model simulation results for the Wyre at St Michaels for the period 23 October to 22 November 1986 (solid line: observed flow; long dashes: predicted total flow; short dashes: predicted "baseflow"; lower dashed line: soil moisture deficit).

and predicted hydrographs for the case of optimised isochrones, first using raingauge and then radar data as rainfall input to the models. Flows predicted using radar data were again slightly better than those obtained from raingauge data. The hydrographs obtained reflect the differences between radar and raingauge measurements in individual events, some rainfall events being well measured by one and not the other.

An analysis of the radar and raingauge data for the first main storm on 27 October 1986 reveals that the raingauge records more than the coincident radar pixel (Figure 5.3.2(a)), after correction for the area of anomaly. The catchment average radar rainfall is lower still (Figure 5.3.2(b)), reflecting a true rainfall gradient across the catchment for this storm. Clearly the presence of the blockage seen in Figure 5.3.3 cannot help the radar assessment of rainfall at this time, although the detail of its effect on the model is complex.

The radar data yielded better flow predictions for both the simple isochrone case and after optimisation of isochrones, though calibration was halted in the case of raingauge data to keep the parameter values within acceptable physical limits. For both radar and raingauge data, optimisation of isochrones clearly results in better flow prediction. Figure 5.3.4 shows the DTM-derived "unit hydrographs" and the time and space response functions of the overall model, with optimised isochrones, are shown in Figure 5.3.5. The double-peaked form of the time response function is a direct consequence of topographic control on travel times in the Wyre catchment. Preliminary work on slope dependent isochrones indicates that the double-peak effect is diminished, but its impact on model performance is still to be assessed.

Addition of distributed stores into the model is seen to make little difference, and in the case of radar data, actually makes predictions worse, though results are slightly improved for raingauge data. Inclusion of urban area delineation into the model formulation has not been tested for the Wyre as it is a predominantly rural catchment. Overall the results show that the use of radar rainfall data results in slightly better flow prediction than that obtained from raingauge data. Clearly further testing of the model needs to be done using different events to get a better idea of model performance under a variety of conditions.

(a) Radar grid value over the Abbeystead gauge

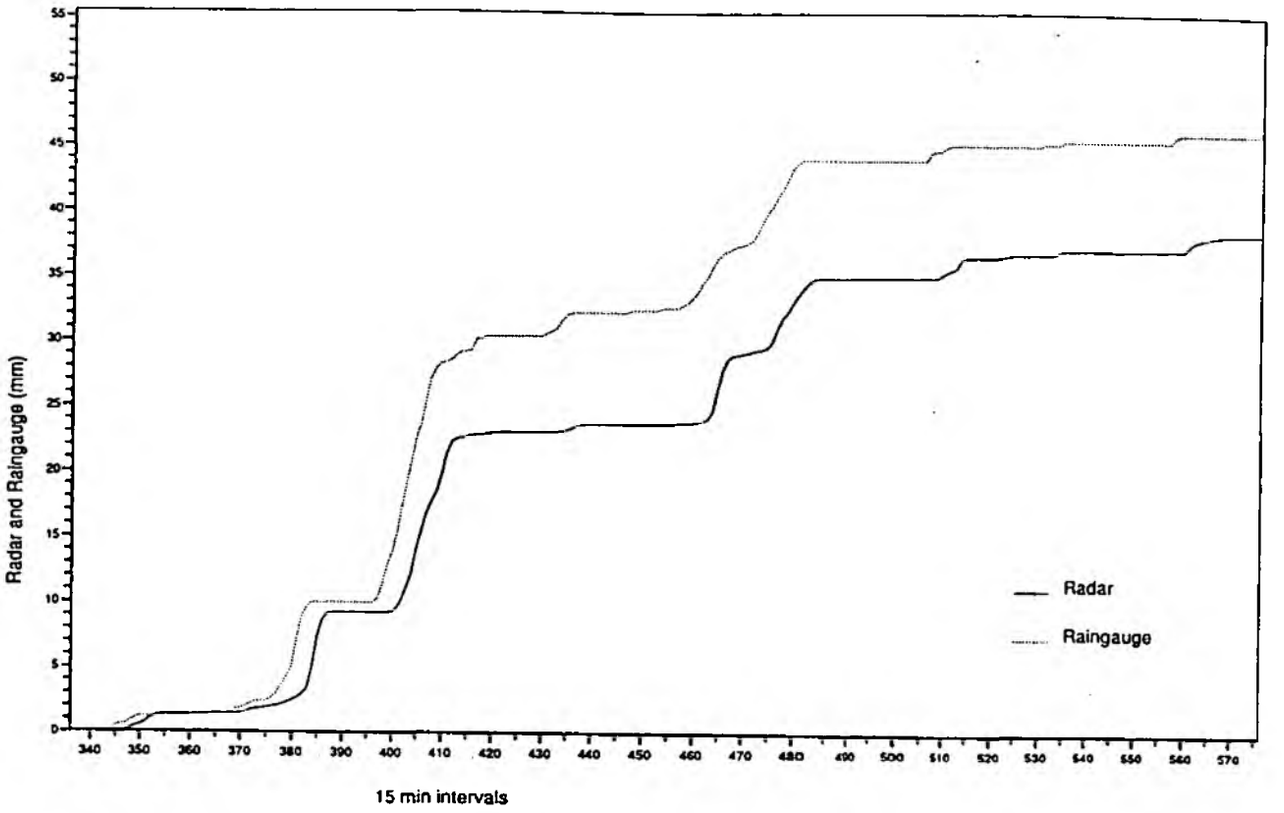

(b) Catchment average radar value

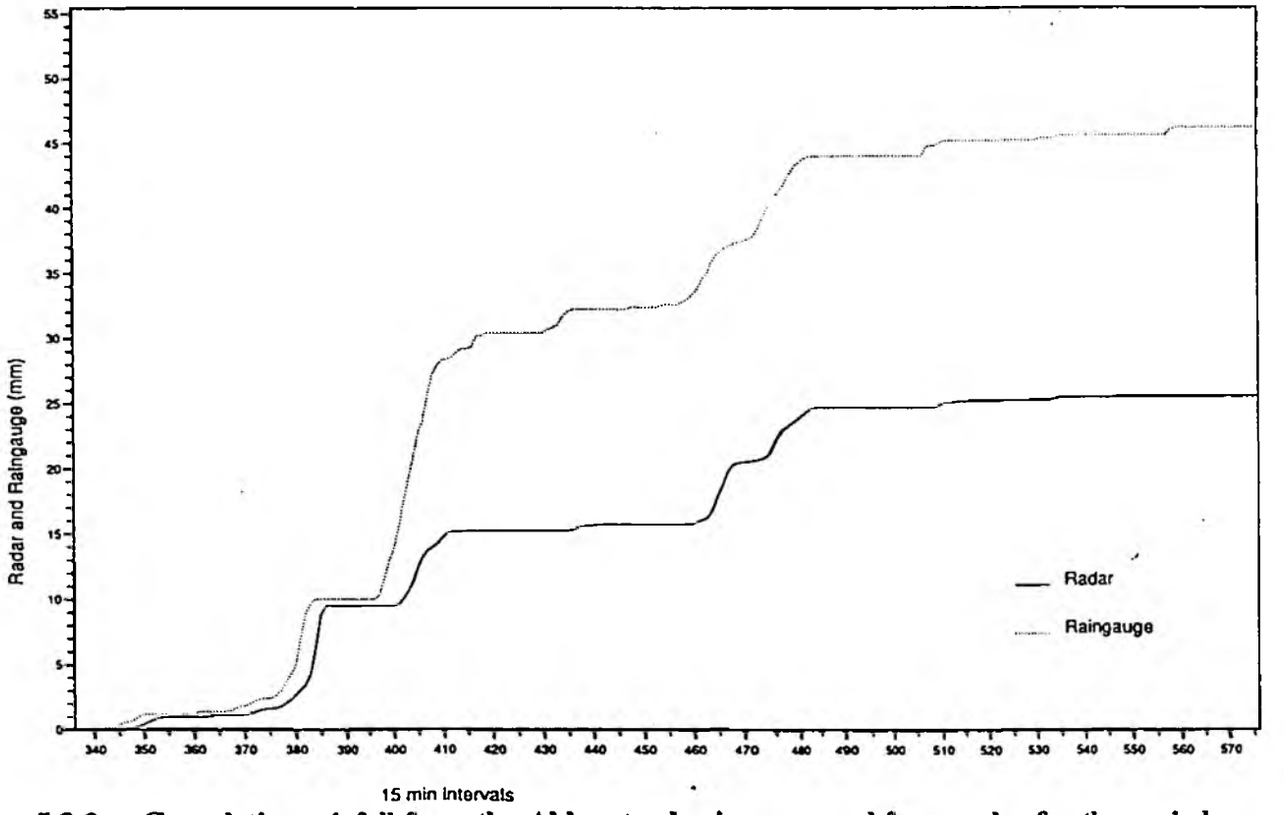

Figure 5.3.2 Cumulative rainfall from the Abbeystead raingauge and from radar for the period 00.00 22 October to 12.00 29 October 1986

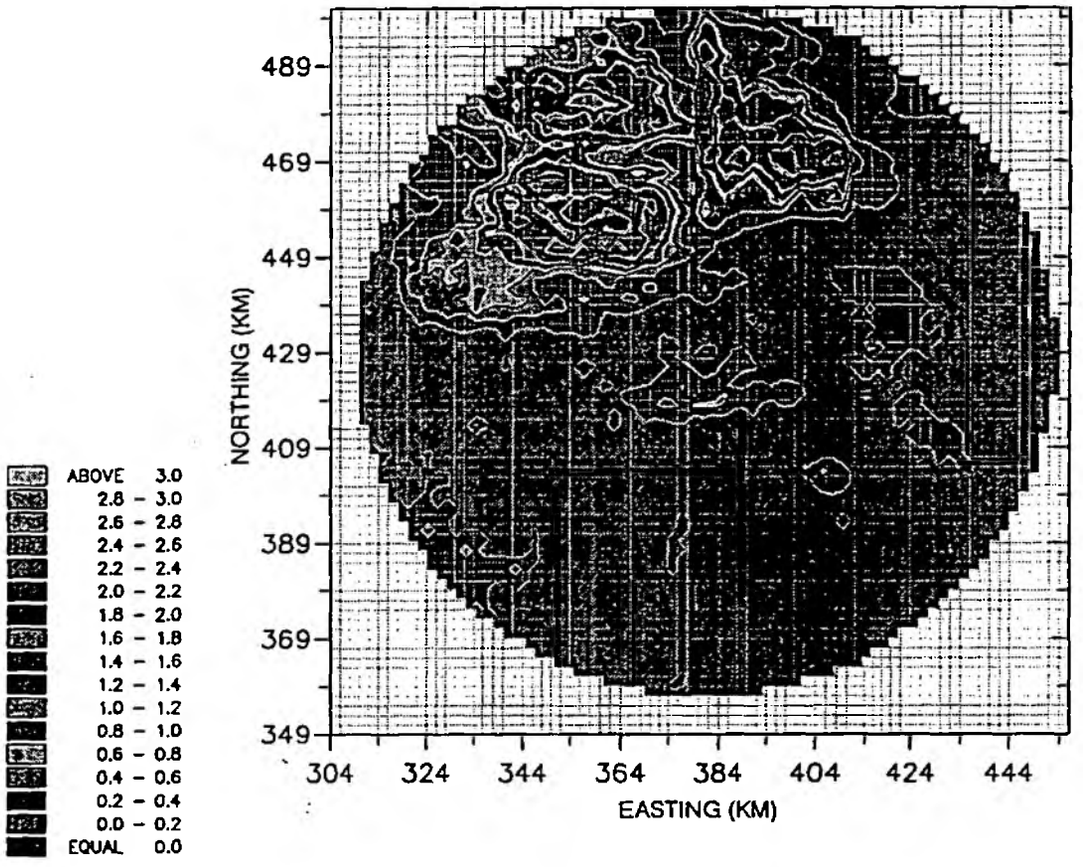

Figure 5.3.3 Hameldon Hill 2 km radar rainfall field (mm h^{-1}), without anomaly removal, averaged over the period 09.00 to 15.00 27 October 1986.

(a) Before optimisation: land velocity = 5 m min^{-1}, river velocity = 30 m min^{-1}

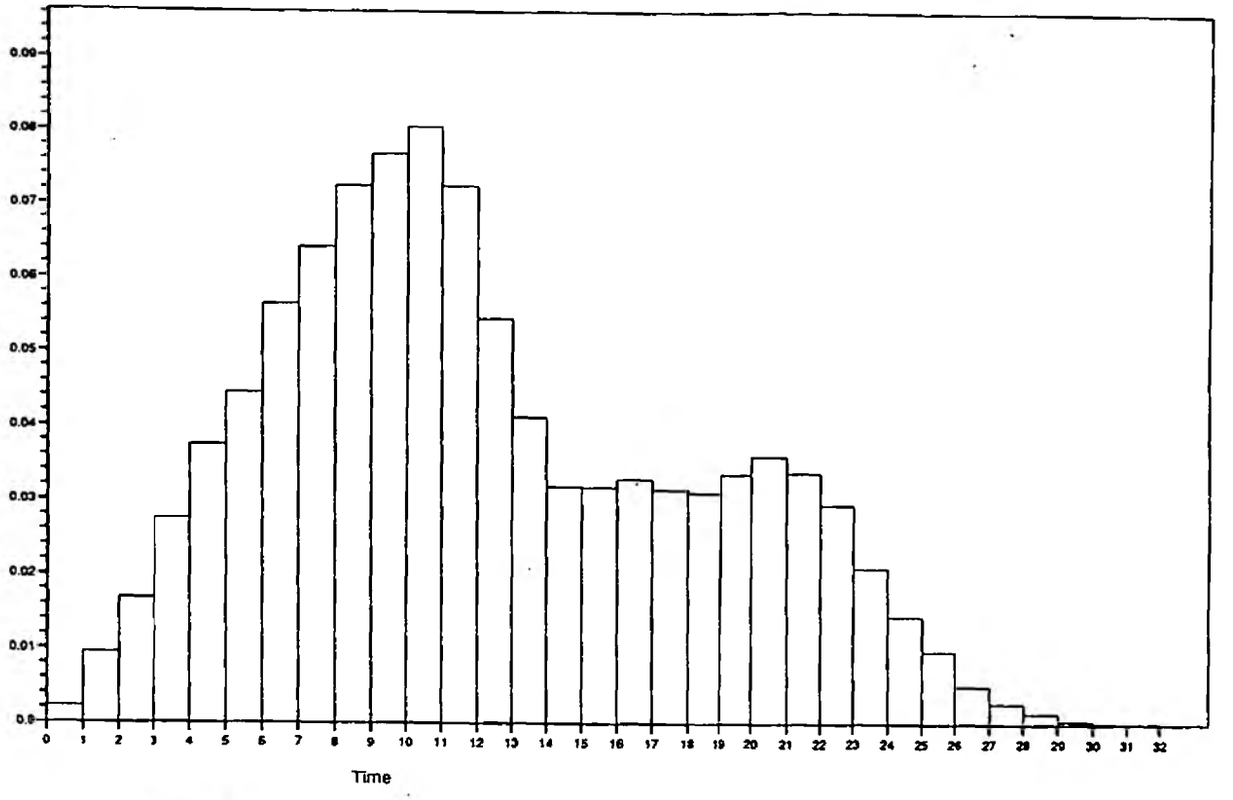

(b) After optimisation: land velocity = 3.215 m min^{-1}, river velocity = 42.69 m min^{-1}

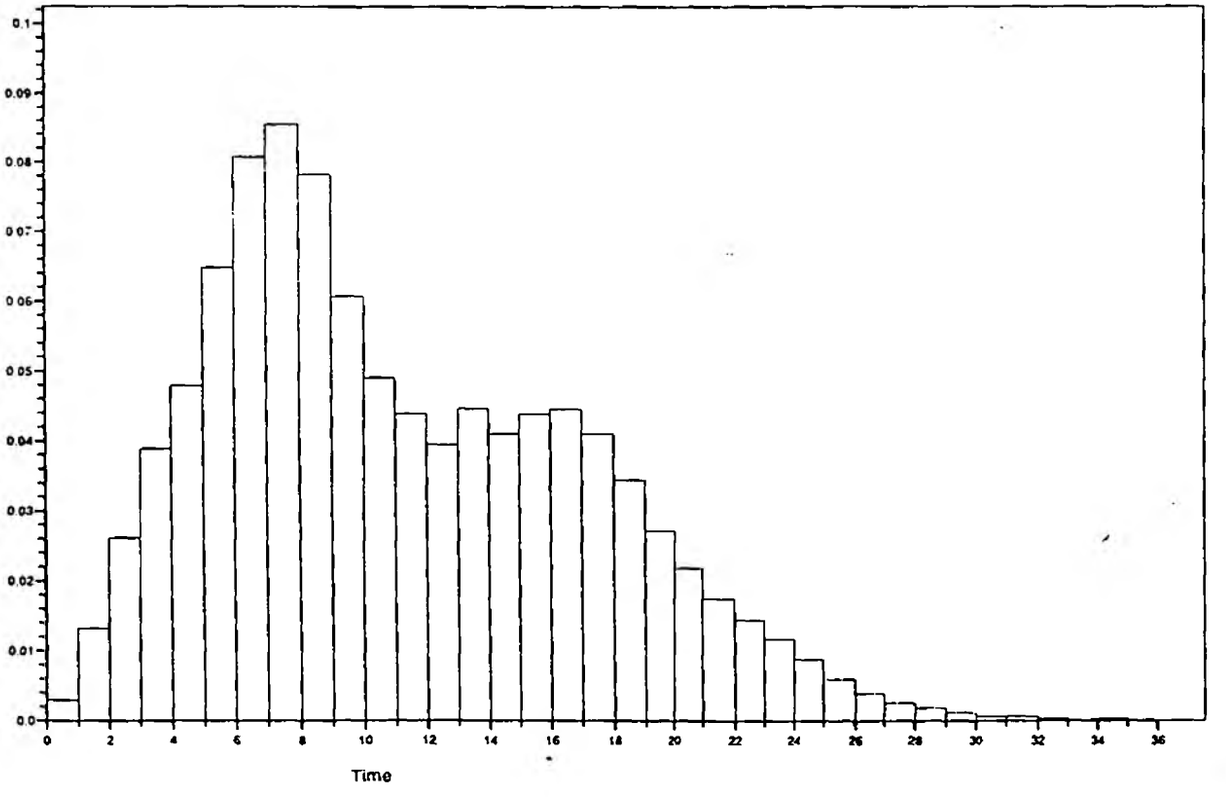

Figure 5.3.4 DTM-derived "unit hydrographs" for the Wyre at St Michaels.

(a) Time response function

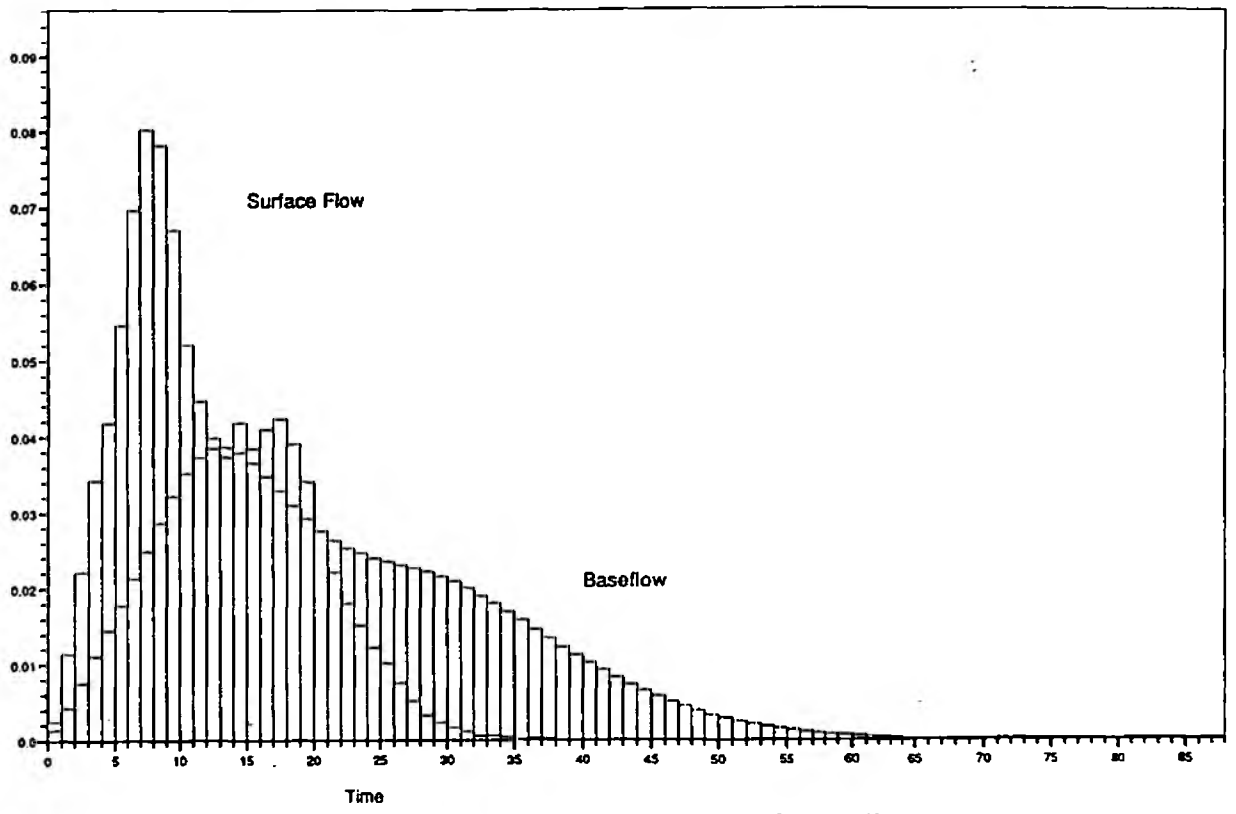

(b) Space response function (fast response only for times 0, 20, 40, 60 hr)

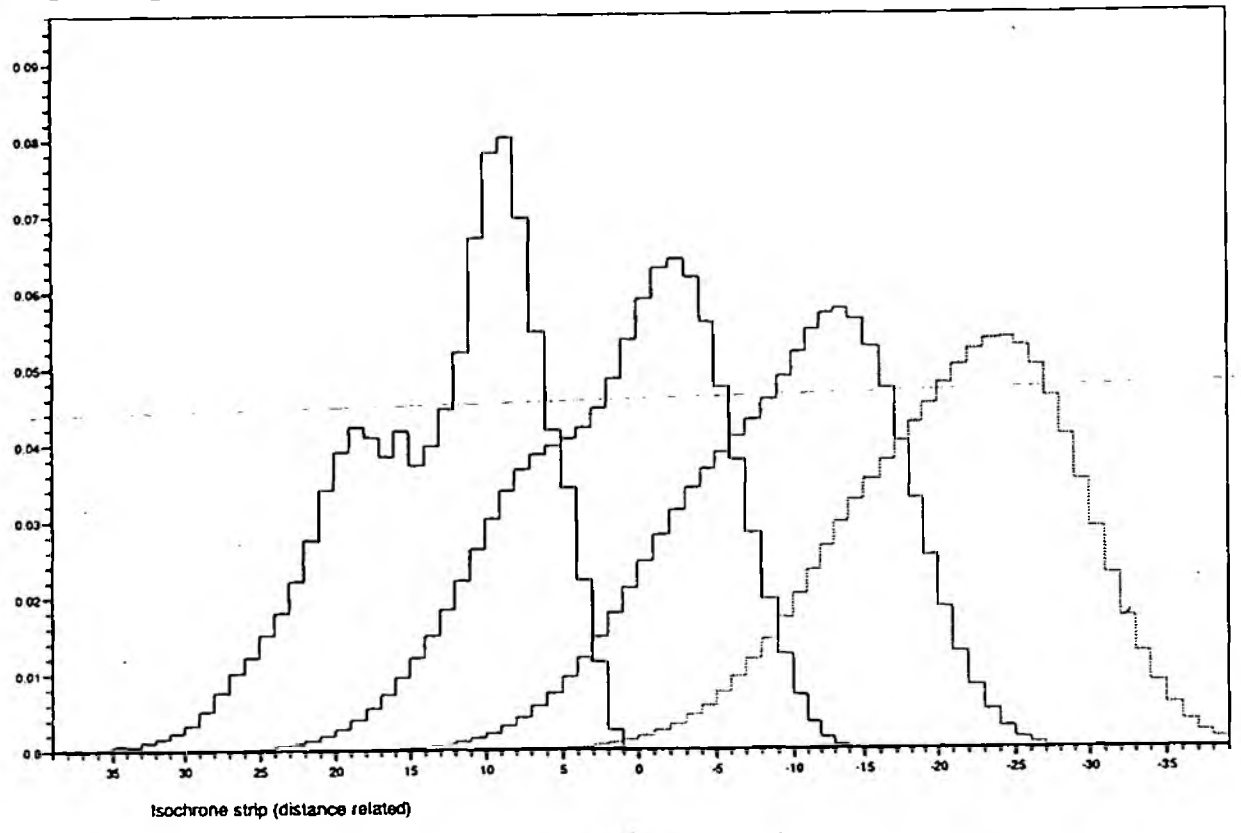

Figure 5.3.5 Model time and space response functions, incorporating time area ("unit hydrograph") and kinematic wave effects, for the Wyre at St Michaels; hourly time step.

6. CONCLUSIONS AND FURTHER WORK

A practical methodology for distributed rainfall-runoff modelling using grid-square radar data has been developed. The problem of over-parameterisation has been circumvented through the use of measurements from a contour map or digital terrain model of the basin together with simple linkage functions. These functions allow many model variables to be prescribed through a small number of regional parameters which can be optimised to obtain a good model fit. Model performance using grid-square radar data has been shown to lead to improved performance, relative to the use of a single raingauge, in a situation where the quality of the weather radar data can be relied upon.

The main developments and conclusions obtained from the Study so far are itemised below:

(i) Development of a "Catchment Climbing" algorithm which automatically infers isochrones from a DTM.

(ii) Formulation of different velocity models for isochrone derivation, including slope dependent forms based on the Chezy-Manning relation.

(iii) Automatic inference of optimal isochrones through incorporating DTM path information within the rainfall-runoff model. This allows flow velocity to be incorporated as a parameter estimated by optimisation along with other model parameters.

(iv) Extension of the basic routing component of the model to incorporate diffusion in addition to a pure advection form of translation.

(v) Replacement of a convolution by a routing operation for flow routing, based on a discretised kinematic wave model, with associated significant savings in computation time.

(vi) Derivation of land cover data from Landsat imagery to support distributed modelling of runoff production through land cover effects on evaporation and effective storage capacity.

(vii) Establishment of an initial database for model calibration and evaluation.

(viii) Preliminary model evaluation results for two of the three Study catchments have demonstrated:-

  (a) A substantial improvement in performance when radar data are used in place of a single raingauge in the 126 km^2 Mole at Kinnersley Manor catchment: 83% explained variance in contrast to only 55%.

  (b) A significant improvement in model performance through incorporating estimation of the velocities for isochrone derivation into the rainfall-runoff model parameter optimisation procedure: 83% explained variance in contrast to the original 73% in the case of the Mole.

(c) A marginal improvement in performance when Landsat-derived urban areas are used to reduce storage capacity: a 2% increase from 83% in the case of Kinnersley Manor.

(d) Further subdivision of the 2 km model grid into smaller grids for soil moisture accounting provides no further improvement.

(e) Problems with blockages in the radar field for Hameldon made the model results difficult to assess. Within the month-long event considered for the Wyre at St. Michaels the raingauge provides the better rainfall estimate for one storm and the radar for another, with both performing about equally overall with 71% of the variance accounted for by the model.

The Study so far has performed model evaluation in "simulation mode" only. In this mode the model acts as a transformation of rainfall (and potential evaporation) into runoff without reference to observed runoff, other than as a basis for assessment. This allows the evaluation to focus on the deterministic model formulation and its shortcomings. Future work will include developing an updating form of the model based on state adjustment, in which the internal water store contents of the model are adjusted using observed runoff values, to achieve better accordance between observed and model forecast values. These results will be compared with an error prediction form of updating which exploits the dependence seen in past model errors to predict future ones: these are then used to improve the initial form of the forecast.

Extension of the database is also planned, and in particular the incorporation of Welsh catchments and Dyfed radar data into the evaluation framework. The strategy adopted up to now has been to use a continuous month of data for both model calibration and assessment. Use of a month of data containing a good number of flood events along with a model with few parameters means that overfitting should not seriously affect the results obtained so far. However, incorporation of further months of data into the database will allow the opportunity for "split-sample testing" in which part of the data are used for calibration and the remainder for assessment. It is also planned to explore the use of HOST soil classification data (Boorman and Hollis, 1990) in the model parameterisation.

A major focus in the project's first-year has been the development of tools to parameterise a distributed model using DTM and Landsat imagery. Less effort has been expended in developing alternative model formulations. In the second, and final year, of the project it is planned to turn the focus more to the model itself and to experiment with different model formulations. Of particular interest will be the performance of these models to make forecasts at sites within and outside the catchments used for calibration, raising the prospect of using the model to forecast at ungauged sites.

REFERENCES

Anderl, B., Attmannspacher, W. and Schultz, G.A. (1976) Accuracy of Reservoir Inflow Forecasts Based on Radar Rainfall Measurements. Water Resources Research, 12(2), 217-223.

Band, L.E. (1986) Topographic Partition of Watersheds with Digital Elevation Models. Water Resources Research, 22(1), 15-24.

Boorman, D.B. and Hollis, J.M. (1990) Hydrology of Soil Types. A hydrologically-based classification of the soils of England and Wales. MAFF Conference of River and Coastal Engineers, Loughborough, UK.

Calkins, D., and Dunne, T. (1970) A Salt Tracing Method for Measuring Channel Velocities in Small Mountain Streams. Journal of Hydrology, 11, 379-392.

Chander, S. and Fattorelli, S. (1991) Adaptive grid-square based geometrically distributed flood forecasting model. In: Cluckie, I. D. and Collier, C. (Eds.), Hydrological Applications of Weather Radar, 424-439, Ellis Horwood.

Emmet, W.W. (1978) Overland Flow. In Kirby, M. J., Hillslope Hydrology. 145-175, Wiley.

Fairfield, J. and Leymarie, P. (1991) Drainage Networks from Grid Digital Elevation Models. Water Resour Res., 27(5): 709-717.

Leopold, L.B., Wolman, M.G., and Miller, J.P. (1964) Fluvial Processes in Geomorphology. W. H. Freeman, San Francisco.

Moore, R.J. (1985) The probability-distributed principle and runoff prediction at point and basin scales, Hydrological Sciences Journal, 30(2), 273-297.

Moore, R.J. (1991) Use of Meteorological Data and Information in Hydrological Forecasting. In: A. Price-Budgen (Ed.), Using Meteorological Information and Products, 377-396, Ellis Horwood.

Moore, R.J. (1992) Grid-square rainfall-runoff modelling for the Wyre catchment in North-West England. Proceedings of the CEC Workshop: Urban/rural application of weather radar for flow forecasting, 3-4 December 1990, Dept. of Hydrology, Soil Physics and Hydraulics, University of Wageningen, The Netherlands, 4pp.

Moore, R.J. and Jones, D.A. (1978) An adapted finite-difference approach in real-time channel flow routing. In: G.C. Vansteenkiste (ed.), Modelling and Control in Environmental Systems, North Holland.

Moore, R.J. and Bell, V. (1993) A grid-square rainfall runoff model for use with weather radar data. Advances in Radar Hydrology, International Workshop, Lisbon, 11-13 November 1991. Commission for the European Communities, 9 pp. In press.

Moore, R.J., Hotchkiss, D.S., Jones, D.A. and Black, K.B. (1991) London Weather Radar Local Rainfall Forecasting Study: Final Report, Contract report to the National Rives Authority, Thames Region, September 1991.

Morris, D.G. and Heerbegen, R.G. (1988) Automatically Derived Catchment Boundaries and Channel Networks and their Hydrological Applications. Geomorphology, 1:131-141.

Morris, D.G. and Flavin, R.W. (1990) A Digital Terrain Model for Hydrology. Proceedings of the 4th International Symposium on Spatial Data Handling, Zurich, 1:250-262.

Pilgrim, S. (1976) Travel Times and Nonlinearity of Flood Runoff From Tracer Measurements on a Small Watershed. Water Resources Research, 12(3), 487-496.

Pilgrim, D.H. (1977) Isochrones of Travel Time and Distribution of Flood Storage From a Tracer Study on a Small Watershed. Water Resources Research, 13(3), 587-595.

Polarski, M. (1992) A review of conceptual rainfall-runoff models using digitally distributed data, Report to MAFF, Institute of Hydrology, 36pp.

Roberts, G.A., M. France and Robinson, R. (1992) Computing the water balance of a small agricultural catchment in southern England by consideration of different land use types. I. Land classification using remotely-sensed imagery, Agric. Water Management, 21, 145-154.

Roberts, G. and Roberts, A. (1992) Computing the water balance of a small agricultural catchment in southern England by consideration of different land use types. II. Evaporative losses from different vegetation types, Agric. Water Management, 21, 155-166.

Tarboton, D.G., Bras, L.R. and Rodriguez-Iturbe, I (1989) Scaling and Elevation in River Networks. Water Resources Research, 25(9), 2037-2051.

A. THE DIGITAL TERRAIN MODEL

A.1 Introduction

This project has made use of the first release of the Institute of Hydrology's hydrological digital terrain model (IHDTM). The IHDTM consists of five square grids of data consisting of surface type, ground elevation, outflow direction, inflow pattern and cumulative catchment area. A 50 m grid interval is used with points lying on integer multiples of 50 on the GB National Grid (Irish Grid for Ireland). The first release of the model is now available for Northern Ireland, Wales, most of England and part of southern Scotland.

This section describes the design objectives and construction techniques which have been used to create these five grids. Looking forward, it will outline future developments which will be incorporated into later releases of the IHDTM.

A.2 The Five Data Grids

Surface type. Each grid point is allocated to one of the following surface types: sea, land, lake or river. The value at a grid point does not refer to the surface type at the point itself but to the most hydrologically significant type in the 50 m square centred on the grid point where increasing order of hydrological significance is defined to be: land, river, lake, sea. This avoids the fragmentation of important hydrological features such as narrow estuaries and lakes, and ensures that rivers are fully represented.

Ground elevation. The elevation of each grid point, relative to Ordnance Datum, is held to a resolution of 100 mm. If the surface type is land then the elevation is that at the grid point. If the surface type is lake or sea then the elevation relates to the lake or sea even if the point itself is on land (for consistency with surface type). If the surface type is river then the elevation is that of the lowest point on any river within the 50 m square centred on the point.

Outflow direction. Each grid point is allocated an outflowing drainage direction which points to one of its eight near neighbours on the basis of steepest gradient. As described later, outflow directions are imposed on 'sink' points (local lows) to ensure there is always a path from any grid point to the sea.

Inflow drainage pattern. This is derived directly from the outflow directions. Each grid point consists of a number representing which of its eight near neighbours drain towards it.

Cumulative catchment area. Every point on the IHDTM is deemed to have an associated local catchment area of 1 unit, representing its own 50 m x 50 m square, an area of 1/400 km^2. The cumulative catchment area at a point is the sum of the number of units draining through the point including that of its own square. Thus a point with a value of 1 is a source and one with a value of 400 has a cumulative catchment area of 1 km^2.

A.3 Design Objectives

The IHDTM has been constructed to meet the following objectives, not all of which are independent. (Note that all objectives are subject to the limitation that accuracy cannot

exceed the grid interval of 50 m.

- Represent the direction of surface drainage using a 50 m square grid in a way which is consistent with the river network depicted on Ordnance Survey 1:50000 second series maps.

- Allow rapid, accurate and consistent automatic catchment boundary definition to any point on the 50 m grid.

- Allow the likely flowpath to be traced from any point to the sea, and identify where it enters a permanent watercourse.

- Produce acceptable lateral and longitudinal river valley profiles.

- Express elevation to a resolution of 100 mm to allow minor topographical features of hydrological significance to be represented and to allow the depiction of finely-stepped river profiles.

- Minimise errors originating in the source data.

- Whilst starting entirely from a database of digital 1:50000 map data with an initial objective of replacing the manual analysis procedures formerly applied to these maps, the new techniques should be capable of benefiting from more precise data and additional types of data from other sources. Examples include additional contour data, ridge positions and details of the fall in river level over a weir.

A.4 Source Data

The first release of the IHDTM is being constructed entirely from data digitised from 1:50000 maps.

For Great Britain these comprise contours (10 m vertical interval except in areas of extreme relief), lake shores with elevation, high water mark, spot heights from some hill tops, and the river network. The river data have been digitised to IH specifications, mainly in a series of collaborative ventures with the water industry, and organised into a structured network. The other data types are leased from the Ordnance Survey who market them as their 1:50000 CONTOUR digital data set. With the exception of the rivers of the North West NRA region which consist only of the main rivers from the first series maps, and some omitted lowland field drains, all the data have been digitised in full from second series maps.

All Northern Ireland data have been supplied directly by Ordnance Survey (Northern Ireland). Although very similar to the GB data they differ in including the majority of spot heights. With the exception of the spot heights and most of the river network, both of which have been digitised manually, the data has been captured by automatic scanner. In all cases, nominal digitising accuracy is 0.25 mm (12.5 m on the ground) or better.

The volume of data is large. For the UK excluding central and northern Scotland (not yet loaded), there are 36 million pairs of contour coordinates, 6.7 million pairs of river coordinates, 0.3 million pairs of high water mark coordinates and 15 thousand spot heights.

A.5 Data Validation

There are many potential sources of error in digital map data, and even a very small error rate in a set of 43 million data points will cause many errors.

The main types of error, with preferred remedial action, are listed below. It should be noted that in many cases the effect on the IHDTM, if no remedial action is taken, is only slight.

River network errors

Type: Canal coded as a river.
Effect: Serious effect on drainage pattern in flat regions, particularly if the canal crosses a major watershed.
Remedy: Recode as type canal.

Type: Man-made diversionary channel coded as a river.
Effect: Similar to canal coded as river.
Remedy: Recode as 'surface pipe'[1].

Type: Illogical network structure, for example two or more stretches flowing to a point but no stretches leaving.
Effect: The DTM may not route flow along the mapped path of the river.
Remedy: If one of the stretches has been digitised in the wrong direction, reverse it.

Contour data errors (also apply to lake shores and coastline)

Type: Incorrect height.
Effect: Depends on sign and magnitude of error. Relief is also important: in gently sloping terrain the contour spacing is wide so a bad contour will affect more grid points. Deep depressions are the most serious, but are also the easiest to detect.
Remedy: Detect and correct.

Type: Poor edge matching (due to contours not meeting at the edges of published OS GB 1:50000 maps; discrepancy can be a few mm).
Effect: Can produce a step in the elevation grid which in turn can affect the outflow directions. It can be visually disconcerting but its effect on applications is usually trivial. It can be more serious in the case of lake shores or coastline as it makes surface type determination more difficult.
Remedy: Apply automatic edge matching software to merge lines which should meet.

Type: Breaks in lines.
Effect: The accuracy of the interpolation method can be reduced by incomplete contour data.

---

[1] Artificial channels used to transmit water, but which are not part of, nor a replacement for, the natural drainage system (for example mill streams or leets) and whose function could from a hydrological viewpoint be replaced by a pipeline are coded as 'surface pipes' and are not allowed to influence the IHDTM.

Remedy: Many breaks are very short. By automatically bridging gaps of less than 20 m (0.4 mm at map scale), most breaks are eliminated.

Misregistration errors

Type: Rivers displaced relative to contours. Due to the two data types being digitised on separate occasions a small relative shift is very common.

Effect: This can cause a river to cross the same contour more than once, giving the impression that it is flowing uphill in places. It can be difficult to allocate sensible elevations to the river.

Remedy: Either apply a systematic shift to the river data or allow for a possible shift when determining river elevations.

A.6 River Heighting

The interpolation method requires, as one of its inputs, heighted digitised rivers, i.e. rivers expressed as a series of (x, y, z) coordinates. The digitised river network is heighted using the following procedure.

1. Record all places where rivers intersect contours, lake shores or high water mark.

2. Where such intersections coincide with an existing (x,y) river coordinate, add the z value, otherwise insert a new (x,y,z) coordinate into the river network.

3. Use the interpolation method (described below) to obtain the elevation of all sources.

4. Calculate and store for every stretch (length of river between adjacent junctions) the distance (along the river) of its upstream end from the sea.

Now for each river system (all stretches draining to a given mouth):

5. Take the sequence of stretches from the most distant source to the sea. Fit a series of curves between the contour crossings to obtain interpolated heights at the intermediate unheighted (x,y) coordinates. To avoid problems due to rivers recrossing the same contour (see misregistration errors) only the most upstream crossing of any given contour elevation is used.

6. Repeat step 5 from the next most distant source down until the river meets a previously heighted stretch. Repeat until all stretches have been heighted.

A.7 High Water Mark Heighting

The High Water Mark (HWM) on Ordnance Survey maps for England, Wales and Northern Ireland is defined as the position of the HWM of an average tide. For Scotland it is the position of the HWM of an average spring tide. Contours in GB are measured relative to Ordnance Datum which is mean sea level at Newlyn in Cornwall and at Malin Head in Northern Ireland. The elevation of the HWM relative to Ordnance Datum varies according to location (with a discontinuity at the Scottish border). In the absence of detailed information it has been necessary to use a single value for HWM elevation, and a value of

Slopes. Wherever possible, a monotonic curve is fitted through four points. The curve is a probability distribution function, fitted by scaling the four points so that the lowest is at (0,0) and the highest (1,1).

Where only three monotonic points are available for fitting, an attempt is made to generate the fourth. If this is not possible, a logarithmic curve is fitted. This is less reliable than the four point curve, and experience has shown that it is safest to average it with the result of a straight-line fit between the inner two points.

When a ray contains only one point as a result of it being the start of a level section, a second point is generated very slightly higher or lower (depending on the slope approaching the point) than the point. A four point curve can then be fitted which will merge smoothly with the level section.

Tops. A top is indicated when the inner points are of equal elevation and are higher than the second points. It is solved by generating the peak position and elevation, then interpolating between this and the relevant two hillside points. The peak position is obtained by extrapolating the slopes of the sides to find their meeting point. The elevation rise is then reduced by a factor of three (because the majority of hills have round or flat, not spiked, tops) to get the estimated peak elevation. Occasionally it must be further reduced for consistency with the contour interval. In the case of hill top contours known to contain a spot height (detected by one of the other ray pairs), the generated peak must stay below it ensuring that the spot height forms the top of the hill. A final point is generated close to and very slightly below the peak and the logistic function is fitted.

Bottoms (troughs/valleys). These are fitted in much the same way as tops, although extrapolation below the level of any spot heights is permitted (as they are unlikely to be local low points). Extrapolation below nominal high water level (3 m) is not permitted unless there exist data to support it (such as a lower contour or spot height). Note that a ray pair passing through a valley containing a river does not fall into this category - it is classified as 'slope to river'.

Convoluted. When a ray pair passes through a 'convoluted' contour, it crosses or comes close to the same elevation on numerous occasions, making estimation of the grid point elevation very difficult. The first task when fitting is to decide whether the grid point is above or below the contour elevation by counting the crossings from the grid point outwards until a contact of a new elevation is encountered.

To estimate the height at the grid point, the local peak/trough is generated using gradients based on those encountered on conclusion of the scan for a new elevation, and a curve of the type used for tops is fitted.

Other types. These are mostly fitted as slopes, with the exception of: between two rivers where interpolation occurs between a river and a generated high point in order to avoid creating a plane between the rivers and similarly between two coastlines (e.g. on a small island or peninsular).

Stage 5: Combining the results from the ray pairs. A weighted average of the elevation estimates from the ray pairs is taken with the greatest weight being given to rays fitted to a

3 m has been taken.

A.8 Derivation of the Surface Type and Ground Elevation Grids

The elevation and surface type at a specified grid reference is determined using an interpolation method. It is applied independently at 50 metre intervals to establish a grid of points. A summary of the method is given here; more detail may be found in Morris & Flavin (1990).

The method has been designed specifically to make use of the properties of the data types from which it is interpolating. It recognises that the coordinates from contour, lake shore, coastline or river represent samples from a continuous feature and that the feature exists between, as well as at, the coordinates. When a river is encountered it is allowed, where appropriate, to dictate the local topography fixing the position of the valley bottom.

The method consists of five stages.

Stage 1: Ray search. A search for elevation information is conducted along a set of an even number of evenly spaced straight lines or rays emanating from the grid point. A ray and its opposite provide a transect passing through the grid point. For each ray, intersections with contours, lake shores, coastline and rivers are recorded up to the distance which provides two intersections of different elevation. A record of any very close, but non-intersecting, lines and spot heights is also made. Additional ray pairs are automatically added if they will pass through important close features, such as spot heights or small closed contours, which would otherwise be missed.

Stage 2: Rationalisation. This prepares the results of the ray search for terrain recognition and curve fitting. Firstly it removes any duplicate information, a common cause of which is multiple copies of the same line segment in the source data. Secondly it flags the onset of any level sections, where a ray runs along a contour.

Stage 3: Terrain recognition. Before a curve can be fitted to a ray pair, the terrain type represented by the intersections must be identified. This determines the fitting technique and affects the weight given to the elevation estimate from the ray pair. The most common types are listed below:

Top	(peak/ridge)
Bottom	(trough/valley)
Convoluted	(repeated crossing of the same contour) between two rivers or coastlines
Slope	- there are several types including:
	Hillside defined by four ascending points
	Slope to spot height
	Slope to river

The surface type is established at this stage, taking the most common type if, due to poor data, not all ray pairs agree.

Stage 4: Fitting. The method depends on the terrain type.

four point slope and of these more weight is given to the steepest. The lowest weight is given to fits between two rivers or coastlines because they are based on an arbitrary gradient.

An important point concerns the number of ray pairs used. It has been shown that reliability of fit increases with increasing number of rays. However, this is at the cost of significant additional computing time. The variations in estimates from the ray pairs can be used to enable the program to adjust automatically the number of rays. Eight ray pairs are used until a point is fitted with excessive variation between ray estimates. When this happens, the point is refitted using twenty ray pairs and then the program continues to use this number for subsequent points until a point is fitted at which there is an acceptably small variation in the twenty estimates.

A.9 The Outflow Grid

The outflow grid can be used to follow the surface flow path from any point to the sea. It is not possible to do this directly from the elevation grid because there is no obvious route from points which have no lower neighbours.

Every point is allocated an outflowing drainage direction, leading to one of its eight near neighbours, as a result of the following procedure.

1. Set directions in lakes by identifying the grid point at the lake outlet and directing towards it, any of its eight near neighbours which are also in the lake. Keep repeating the process for unset lake neighbours of points directed on the preceding pass until all contiguous lake points have been directed.

2. Set the direction of all land and river points according to the steepest gradient. Where two or more directions share the steepest gradient, resolve by comparing inflowing and neighbouring gradients. In flat areas resolve by looking beyond the near neighbours.

3. Where a point represents a local low (termed a sink) resolve by treating as if it was a genuine depression (though they are nearly always artefacts) and use a program to simulate filling it with water until it can overflow and drain to a level lower than the sink (Morris and Heerbegen, 1988). When this spill point is found, reset the sequence of directions to it from the sink.

At all stages ensure that no circular paths are established and that no diagonal paths are allowed to cross.

A.10 The Inflow Grid

During catchment definition it is necessary to know, for each point in the catchment, which of its eight near neighbours drain towards it. This could be determined from the outflow grid, but the process would be inefficient as, on average, each point has only one inflowing neighbour. Major performance benefits are obtained if at each point a single number is stored to represent the distribution of inflowing neighbours.

For each point the outflow direction of each of its eight neighbours is inspected and the

pattern of inward flowing points is coded into an eight bit number.

A.11 The Cumulative Catchment Area Grid

The applications of this grid include:

- Hydrological modelling - it can be used as an aid in the location of watercourses. Drainage networks can be generated where the density is controlled by hydrological conditions, giving an advantage over the digitised 1:50000 river network whose density is fixed by cartographical rules.

- Map production - drainage maps with channel width related to catchment area convey well the structure of the network.

- An aid to interactive applications - when a user points at the screen, this grid can be used to register the input coordinates with the drainage network.

Construction of this grid involves using the outflow grid to trace the flow path from each point to the sea, incrementing the cumulative catchment area of all points traversed. In practice, large efficiencies are made by transmitting accumulated rather than individual values and by originating the process at sources only.

A.12 Future Developments

Some of the improvements planned for later releases of the IHDTM are outlined below.

Comprehensive validation of the source data. Within the schedule for the first release, it has not been possible to undertake all aspects of validation described earlier. In particular, edge matching of contours and reconciling rivers with contours have been deferred.

Heighting the high water mark. The second release of IHDTM will use a HWM which has been heighted using data from the Proudman Oceanographic Laboratory's tidal model instead of the constant 3 m used in the present release. This will give significant improvements in low lying coastal areas and will enable the model to be used to assess the effects of change in sea level. A further improvement here will come from the addition of the 5 m contour from 1:25000 or 1:10000 maps.

Extension to the low water mark. When a digitised low water mark is available, and heighted as described for the HWM, the model will be extended. A new surface type, intertidal will be introduced.

Improved surface type allocation. The present method of allocating type 'sea' or 'lake' when these are present in the 50 m square, but when the grid point is on land, will be replaced by a method which uses the 'square' value only when necessary to preserve the continuity of narrow lakes, estuaries or peninsulas.

Change of ray angles. Currently the eight ray pairs run at angles relative to the east-west line of 0°, 22.5°, 45°, 67.5°, 90°, 112.5°, 135° and 157.5°. Because rays on multiples of 45° pass through neighbouring grid points it is possible for the same ray pair on several

adjacent points to pick up the same intersections. If these represent a very dominant, possibly erroneous, feature, it may result in a linear ridge or trough in the elevation grid. Future versions will avoid this by rotating all ray pairs through half the ray interval (i.e. to 12.25°, 37.75° ..... in the case of eight ray pairs), so that none will lie on 45° multiples.

Direct incorporation of rivers into the outflow direction grid. A preliminary stage will be added to the direction setting procedure to pre-set the directions of the digitised rivers onto the direction grid. This will give improved representation where two rivers are separated by 100 m or less.

Extension of outflow grid into estuaries. It is sometimes necessary to define the total catchment of an estuary, for example the Humber, in which all the contributing rivers do not merge before they reach the sea. A future release will treat estuaries as 'offshore lakes' with directions leading to a single outlet to the open sea.

Improvement to overland flow direction setting. The use of only eight possible flow directions leads to an unnatural occurrence of parallel flow paths with consequent lack of convergence and incorrect routing of flows. This will be corrected by using a method based on that of Fairfield and Leymarie (1991). The slopes at ninety degrees to the steepest gradient will be checked to determine when the steepest direction is not necessarily the most appropriate.

Incorporation of field survey data. Initially for the NRA North West region, watersheds from field surveys will be used to guide the interpolation procedure.

Feedback from users. Development of future releases will take into account any comments received from current uses.